

June 7, 2023

MICROSTRUCTURE-BASED ESTIMATION OF THE EFFECTIVE STIFFNESS OF CROSSLINKED, EMBEDDED FIBER NETWORKS

SB3C 2023
June 4th - 8th, 2023
Vail, Colorado

Sotirios Kakaletsis^{*1}, Emma Lejeune², Manuel K. Rausch¹

¹Aerospace Engineering and Engineering Mechanics, The University of Texas at Austin

²Mechanical Engineering, Boston University

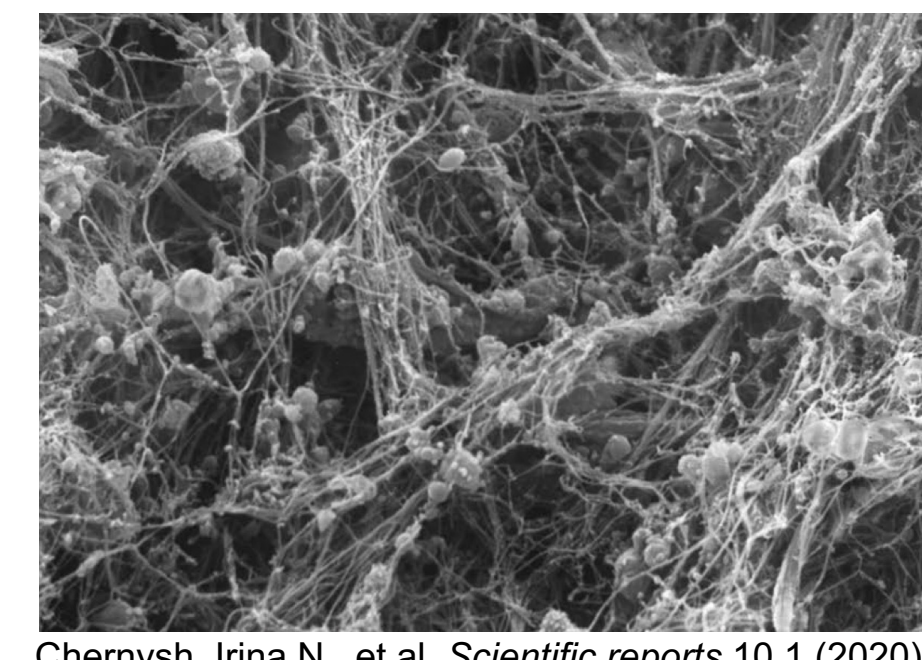
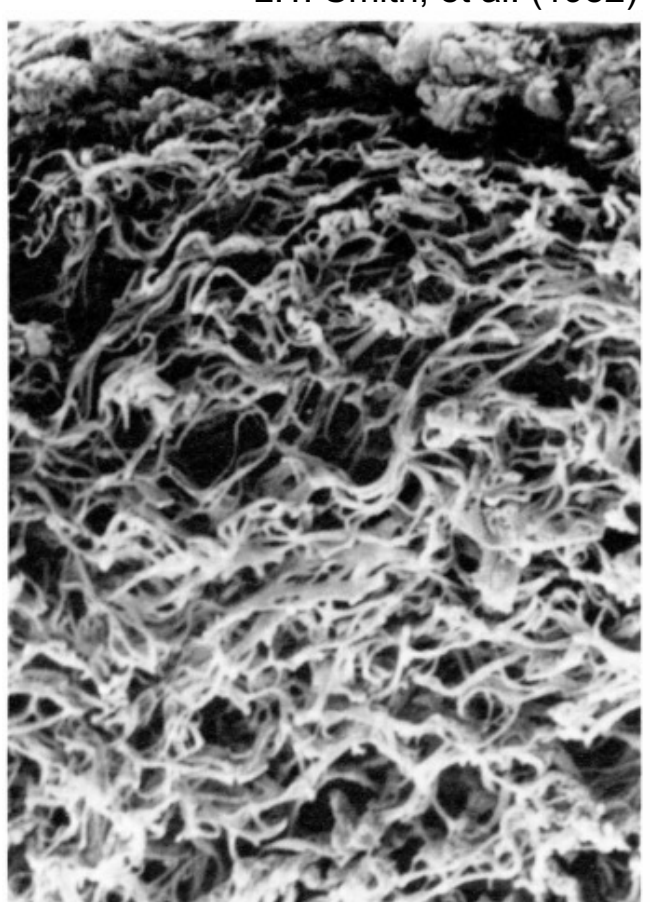
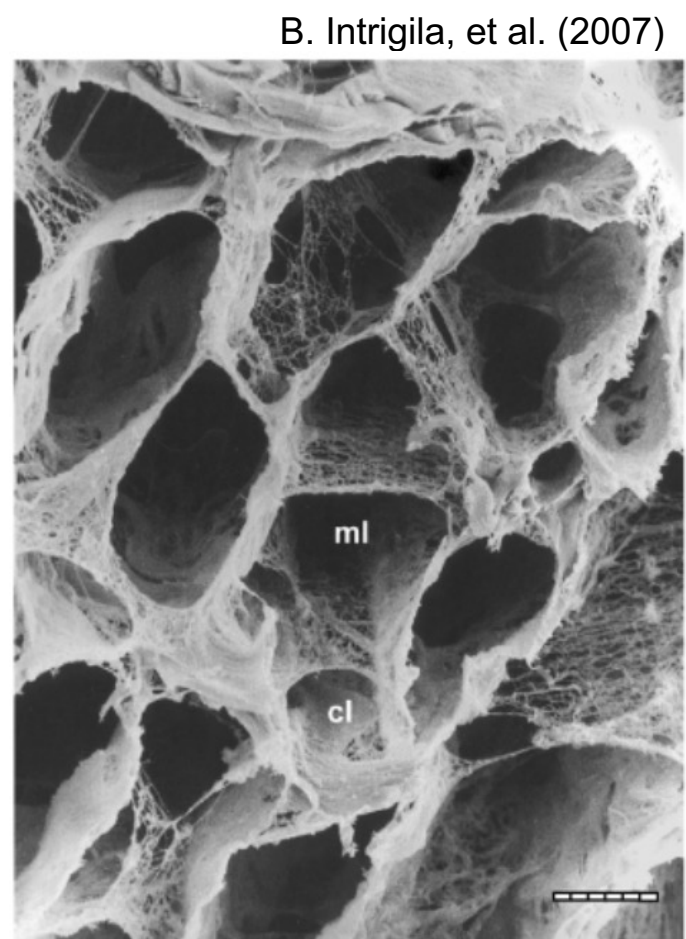
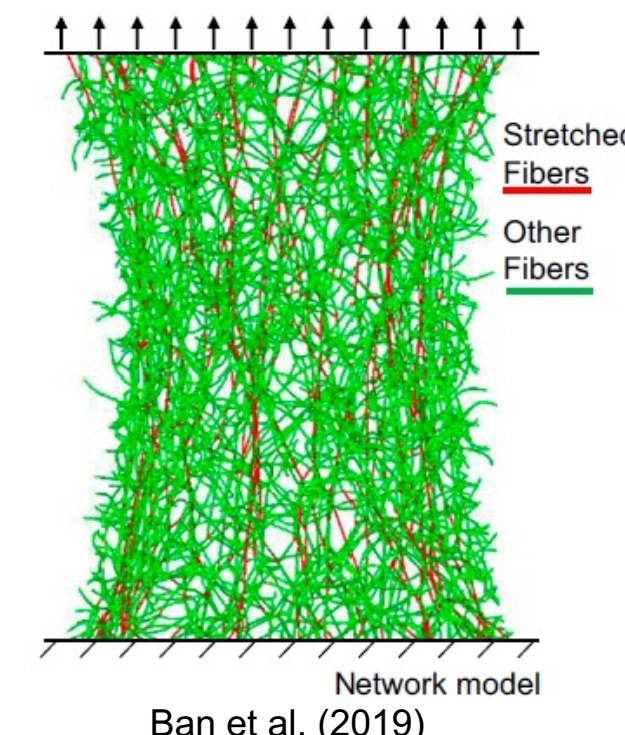
Introduction

- Semi-flexible biopolymers are ubiquitous building blocks of life, often organized in **fibrous networks**
 - Collagen networks in myocardium, skin, blood vessels, ligaments, tendons etc.
 - Fibrin networks in blood clots

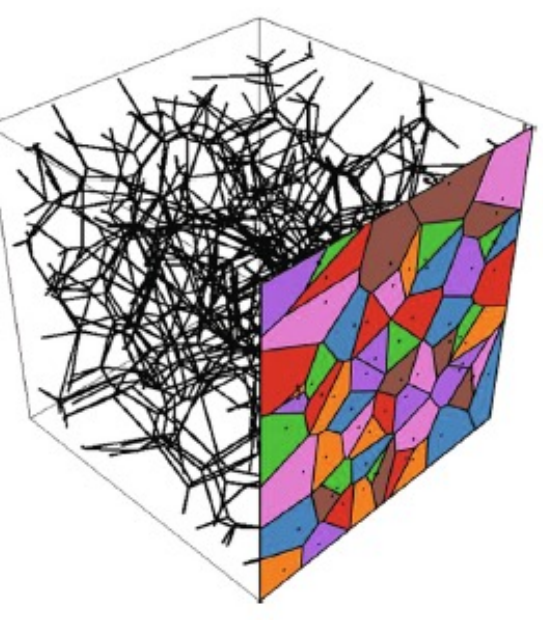
- They exhibit **complex mechanical phenomena**
 - Strong nonlinearities
 - Strain stiffening
 - Anomalous Poisson's effect
 - Negative Poynting effect

- Previous efforts have modeled fiber networks in **isolation**:
 - No embedding matrix
 - Elastic behavior
 - Discrete elements

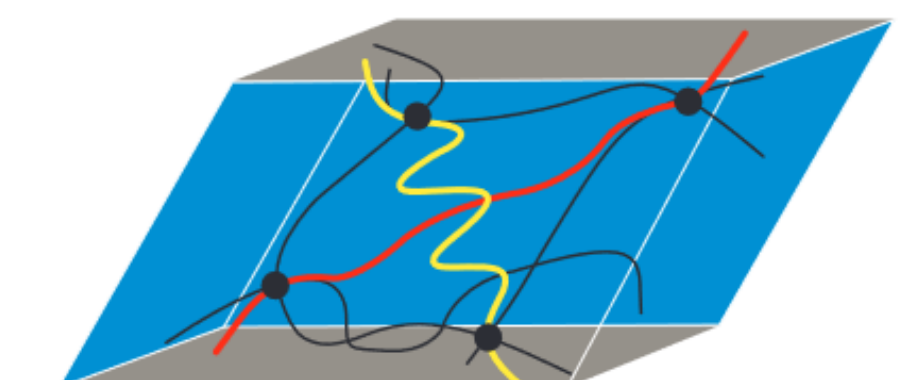
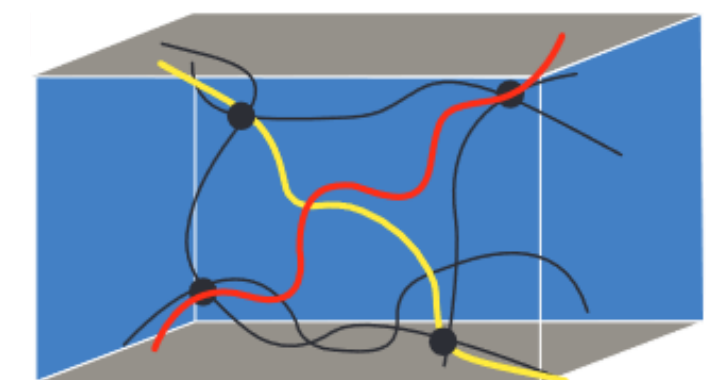
- Why in isolation? – **Discretization**



Chernysh, Irina N., et al. *Scientific reports* 10.1 (2020)



Merson & Picu (2020)



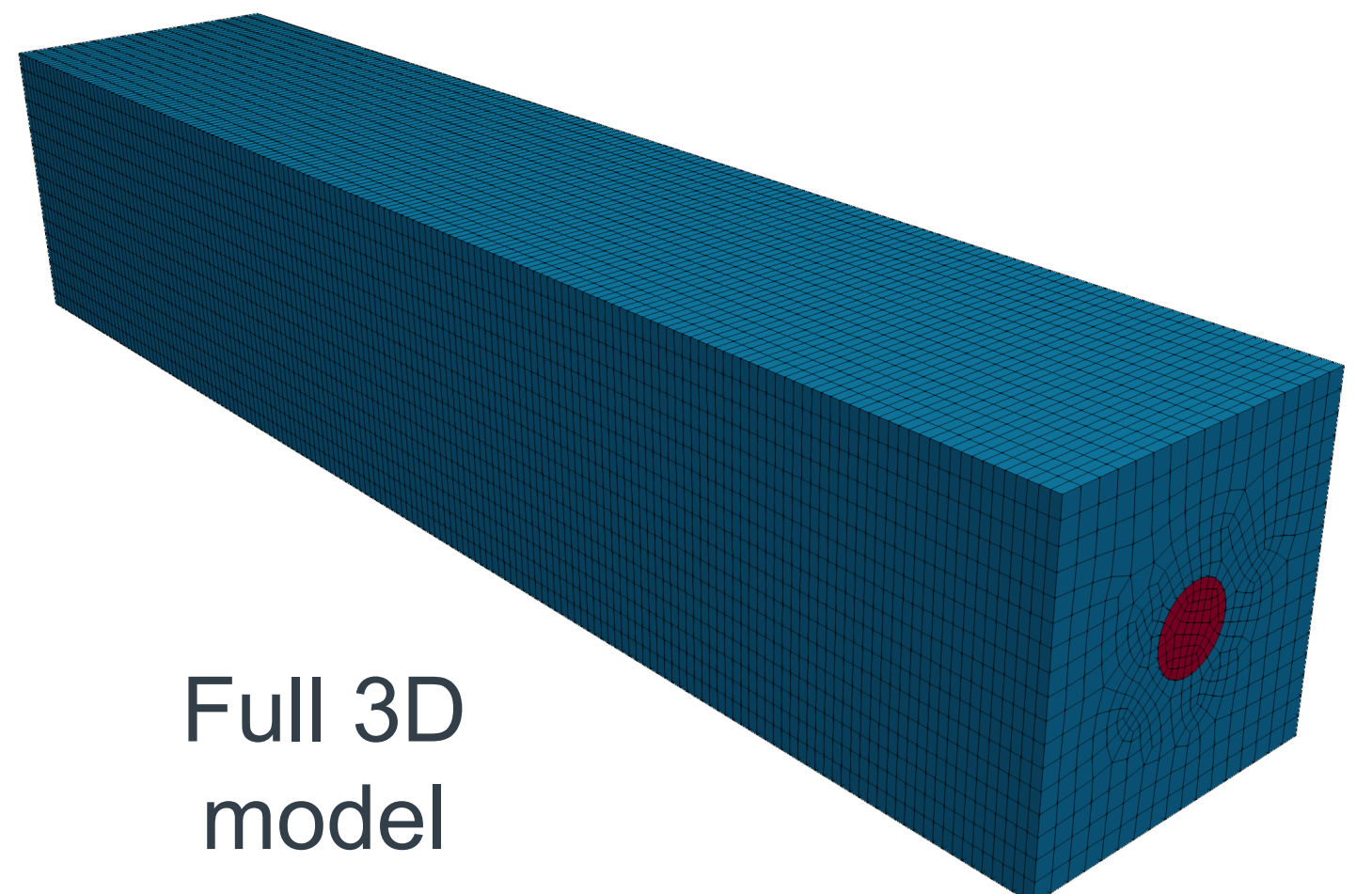
Introduction

- **Motivation:** Delineate contributions of each constituent: **matrix and fibers**

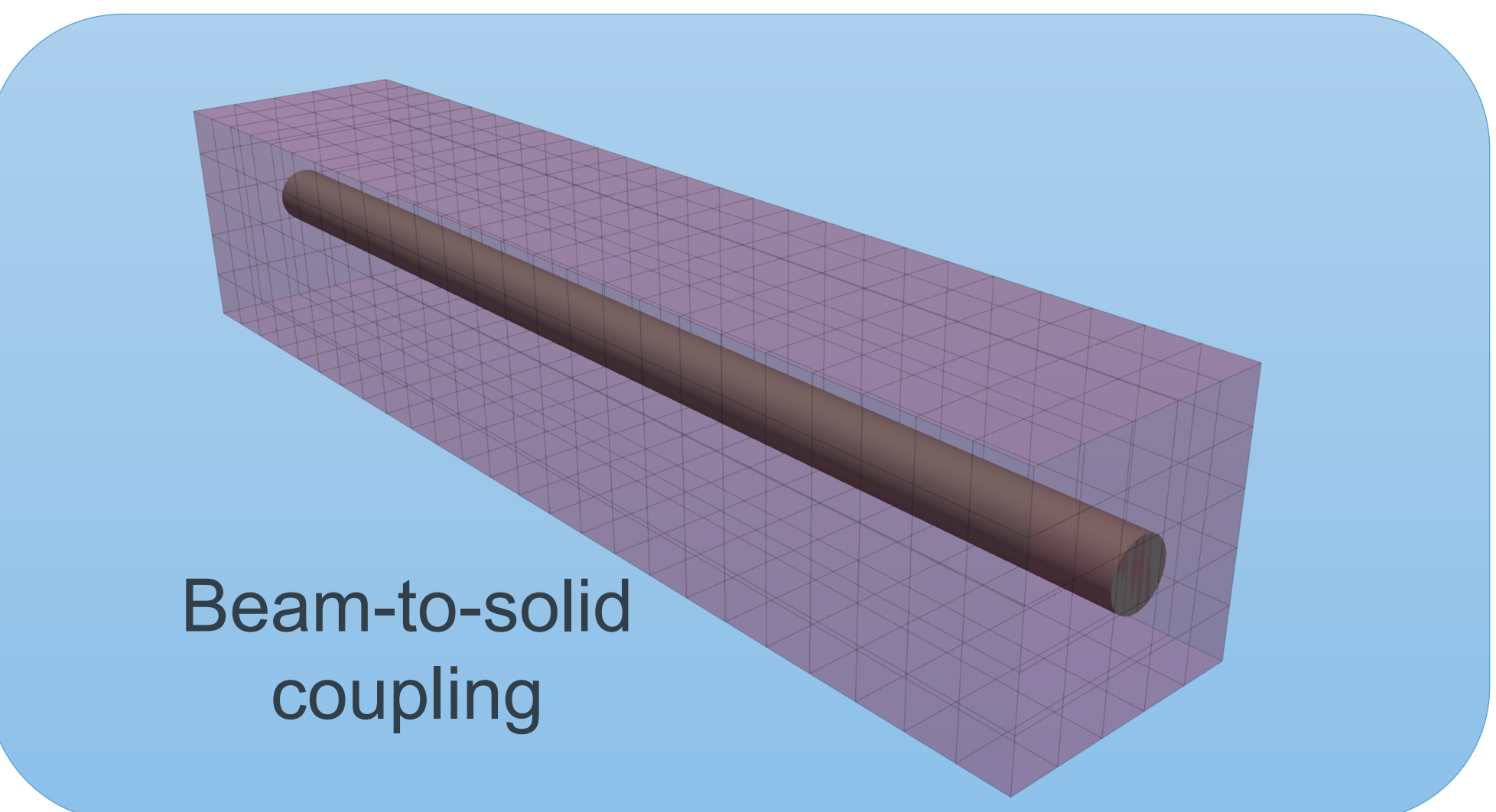
- How does network architecture affect the mechanics/ apparent stiffness?
 - Mean fiber length?
 - Fiber undulations?

- **Objective:** Develop a computationally efficient model of the elastic behavior of embedded fiber networks under large deformation.

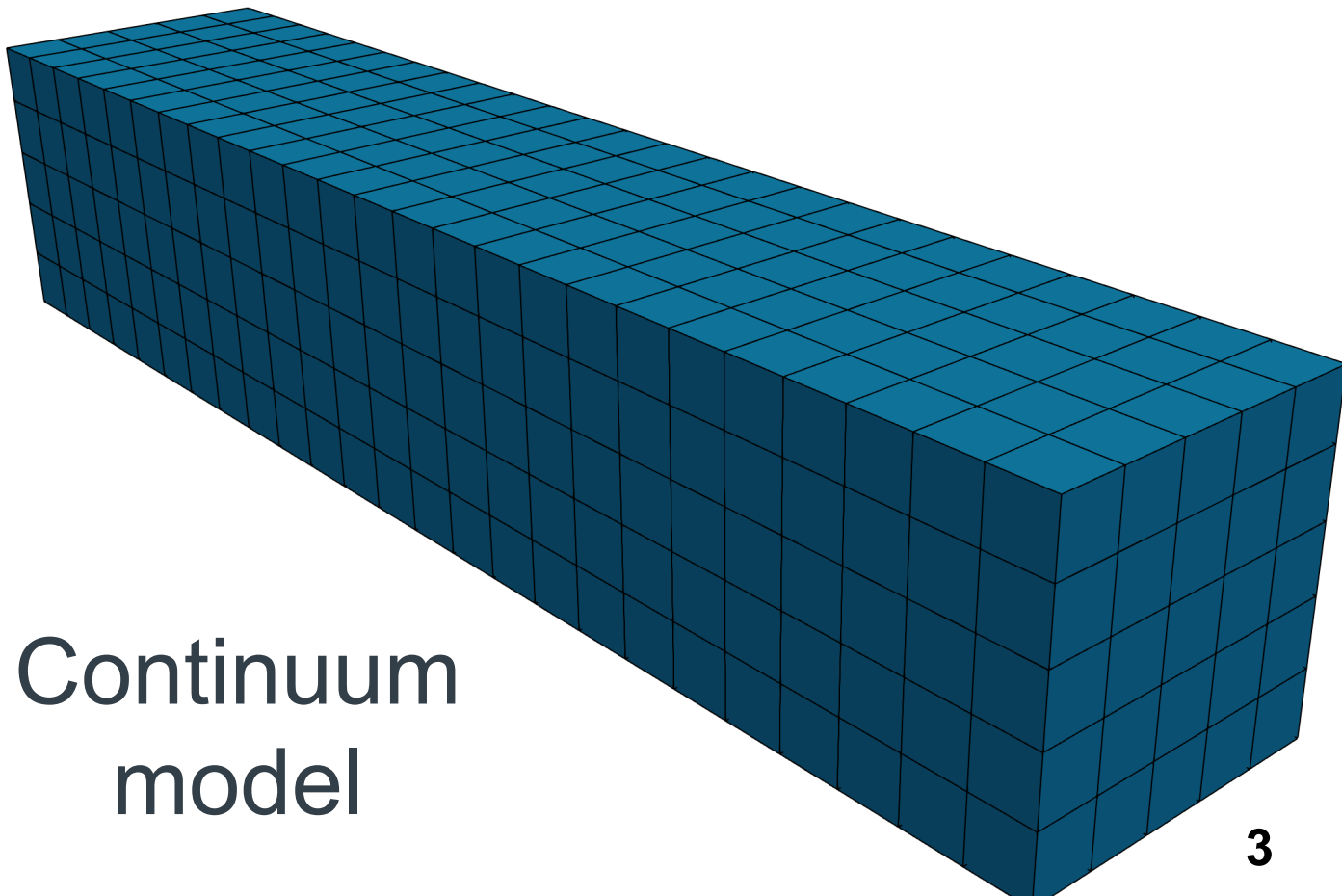
- Modeling approaches for embedded elastic fibers:



Full 3D
model

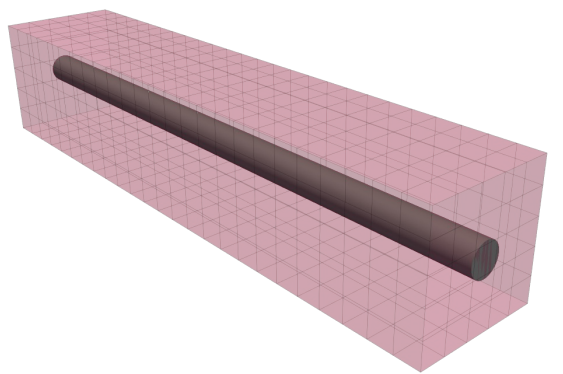


Beam-to-solid
coupling



Continuum
model

Theory



- Based on previous work by Steinbrecher, Ivo, et al. "A mortar-type finite element approach for embedding 1D beams into 3D solid volumes." *Computational Mechanics* (2020).
- Coupling Constraint:

$$\underline{\mathbf{u}}^B - \underline{\mathbf{u}}^S = \underline{\mathbf{0}} \text{ on } \Gamma_c^{1D-3D} = \Omega^B \text{ (beam centerline)}$$

- Principle of virtual work:

Solid Beam Coupling

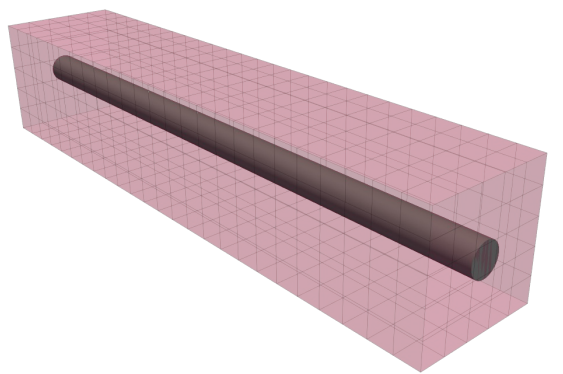
$$\delta W^S + \delta W^B + \delta W^C = 0$$

$$\delta W^C = -\delta W_c + \delta W_\lambda = \int_{\Gamma_c^{1D-3D}} \underline{\lambda} (\delta \underline{\mathbf{u}}^B - \delta \underline{\mathbf{u}}^S) ds + \int_{\Gamma_c^{1D-3D}} \delta \underline{\lambda} (\underline{\mathbf{u}}^B - \underline{\mathbf{u}}^S) ds$$

where

$\underline{\lambda} \in \mathbb{R}^3$: Lagrange multiplier field (interface line load)

Theory



- Linearized system:

$$\begin{bmatrix} K_{SS} & 0 & -M^T \\ 0 & K_{BB} & D^T \\ -M & D & 0 \end{bmatrix} \begin{bmatrix} \Delta d^S \\ \Delta d^B \\ \lambda \end{bmatrix} = \begin{bmatrix} -f_{int}^S + f_{ext}^S \\ -f_{int}^B + f_{ext}^B \\ g_c \end{bmatrix} \quad \text{where } g_c(d^S, d^B) = [-M \quad D] \begin{bmatrix} d^S \\ d^B \end{bmatrix}$$

- Enforce coupling constraint using the penalty method and setting $\lambda = \varepsilon \kappa^{-1} g_c(d^S, d^B)$

$$\begin{bmatrix} K_{SS} + \varepsilon M^T \kappa^{-1} M & -\varepsilon M^T \kappa^{-1} D \\ -\varepsilon D^T \kappa^{-1} M & K_{BB} + \varepsilon D^T \kappa^{-1} D \end{bmatrix} \begin{bmatrix} \Delta d^S \\ \Delta d^B \end{bmatrix} = \begin{bmatrix} -f_{int}^S + f_{ext}^S - f_c^S \\ -f_{int}^B + f_{ext}^B - f_c^B \end{bmatrix}$$

with

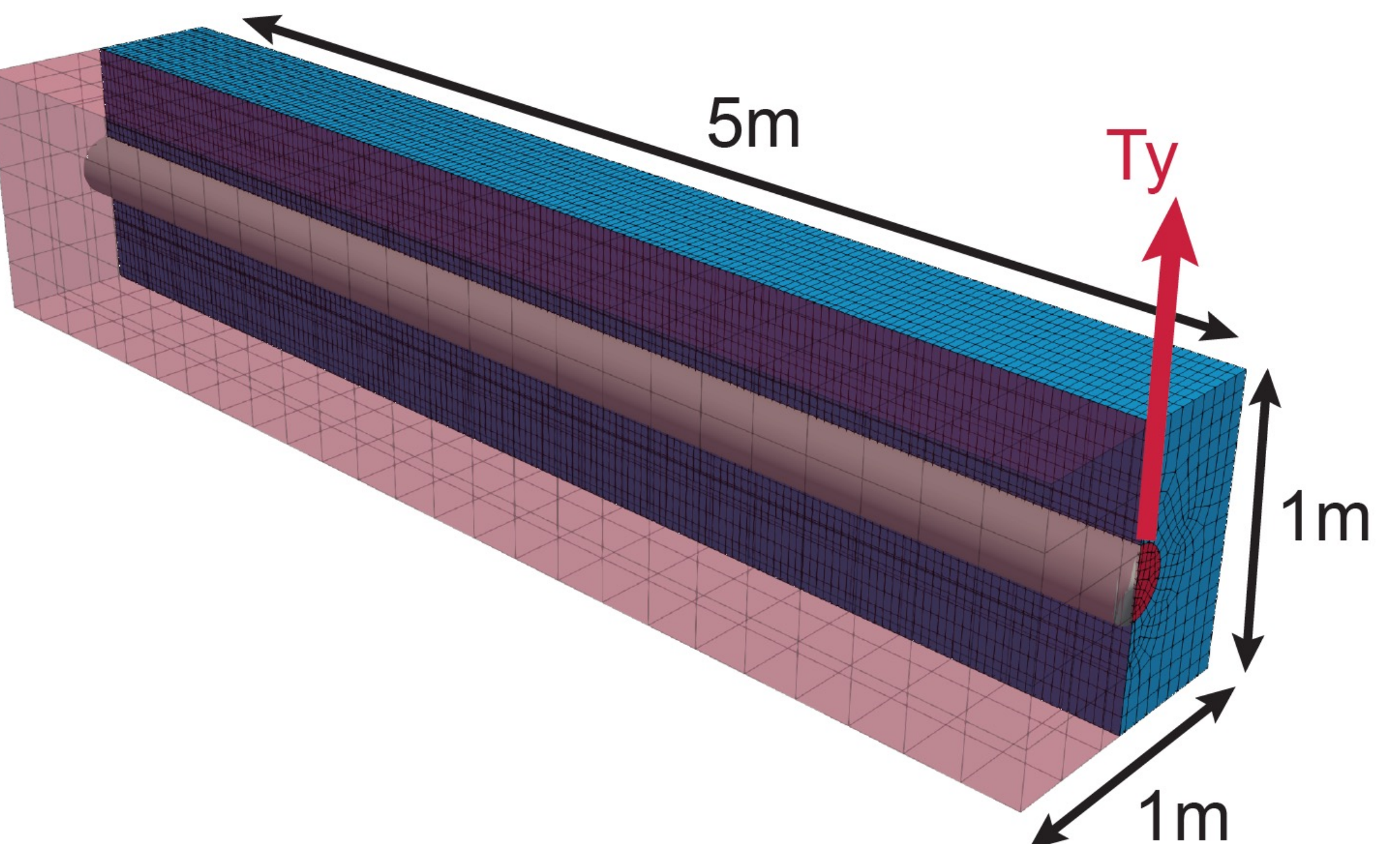
$$-f_c^S = \varepsilon M^T \kappa^{-1} [-M \quad D] \begin{bmatrix} d^S \\ d^B \end{bmatrix}$$

$$-f_c^B = \varepsilon D^T \kappa^{-1} [-M \quad D] \begin{bmatrix} d^S \\ d^B \end{bmatrix}$$

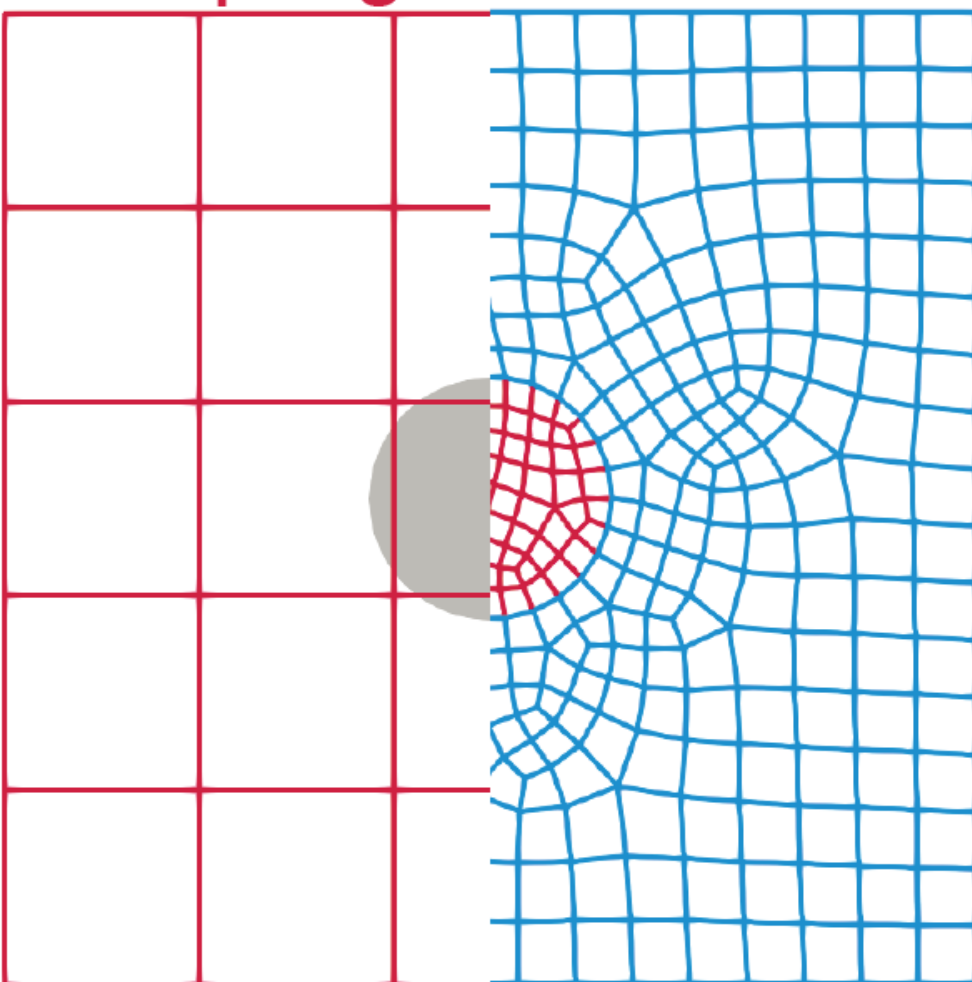
Validation

- Reinforced cantilever beam, fixed on the left end, applied distributed load on the free face (right end).
- Comparison between the full 3D model (reference solution) and our beam-to-solid coupling Abaqus implementation.
- Displacement error of the solid domain:

$$\|e\| = \sqrt{\frac{\int_{V_0} \|\underline{u}^S - \underline{u}_{ref}^S\|^2 dV_0}{\int_{V_0} \|\underline{u}_{ref}^S\|^2 dV_0}}$$

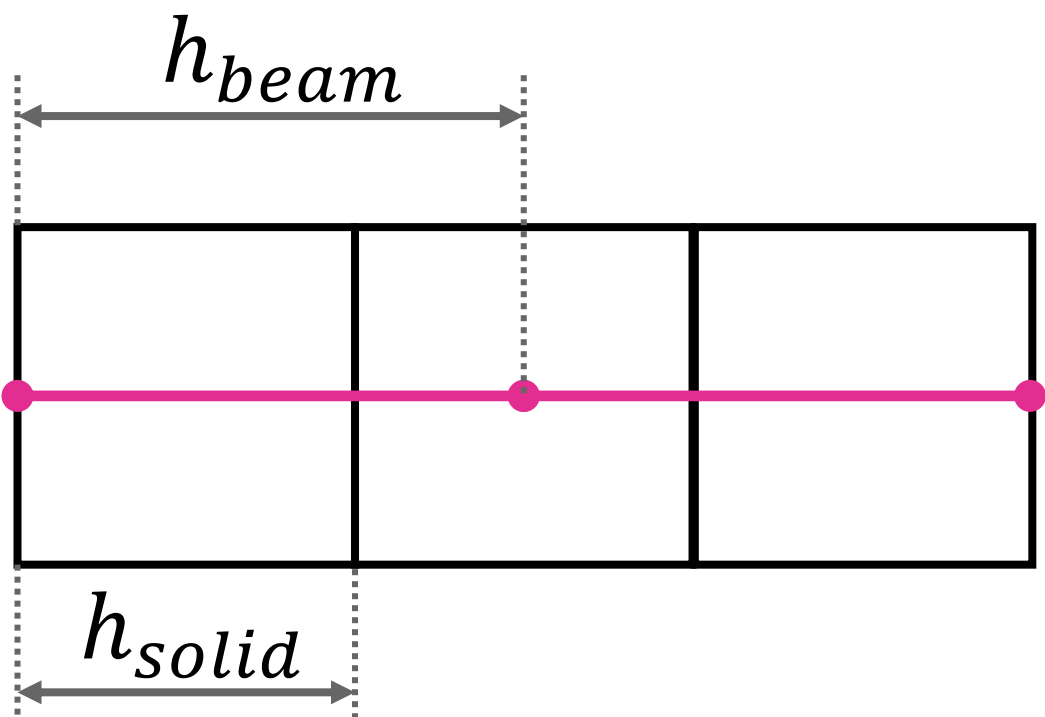


Beam-to-solid
Coupling Validation



Validation – Sensitivity Studies

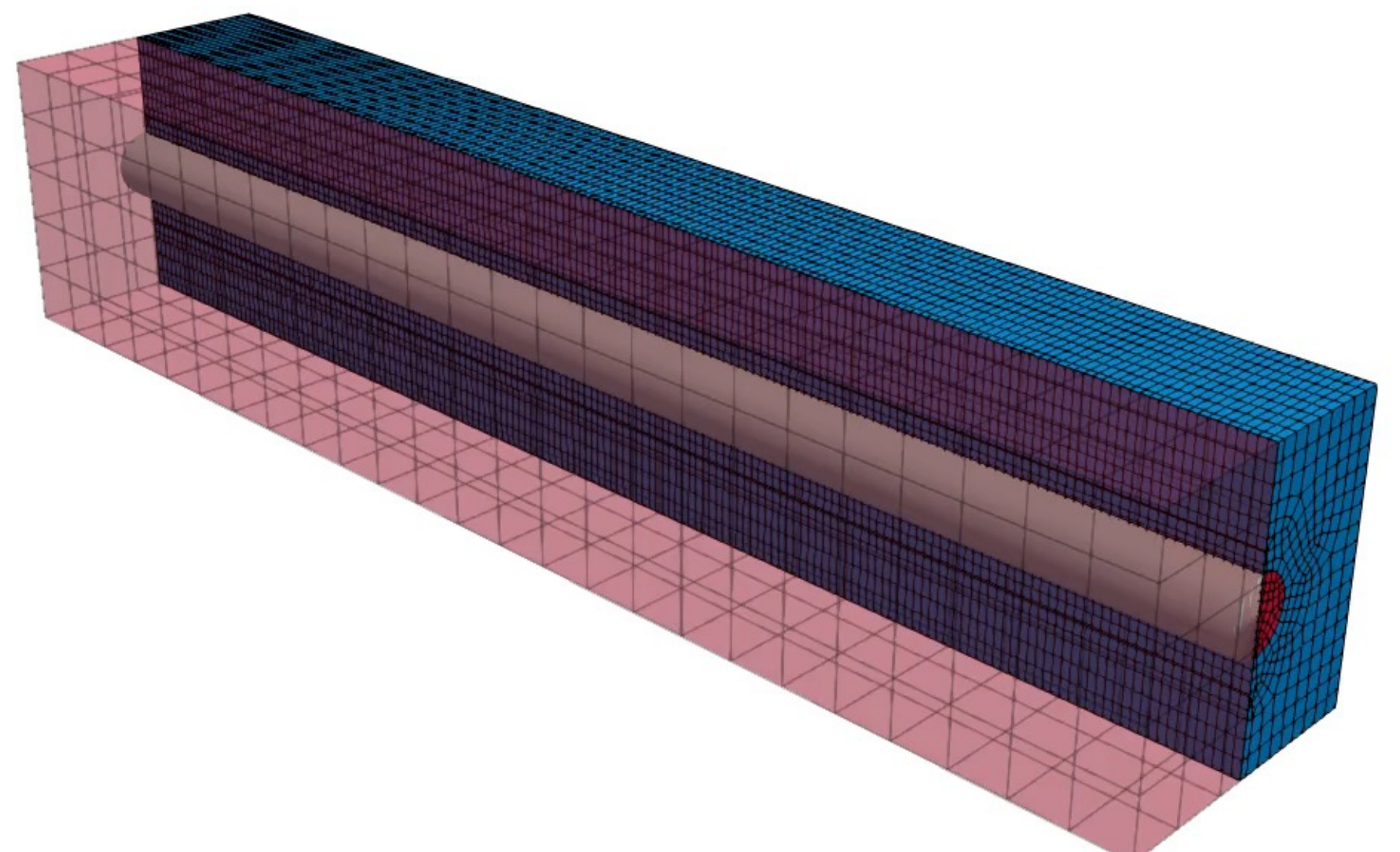
- Limitations
 - Beam element size > Solid element size
 - Solid element size \approx Fiber radius



- Displacement error: < 1.0%

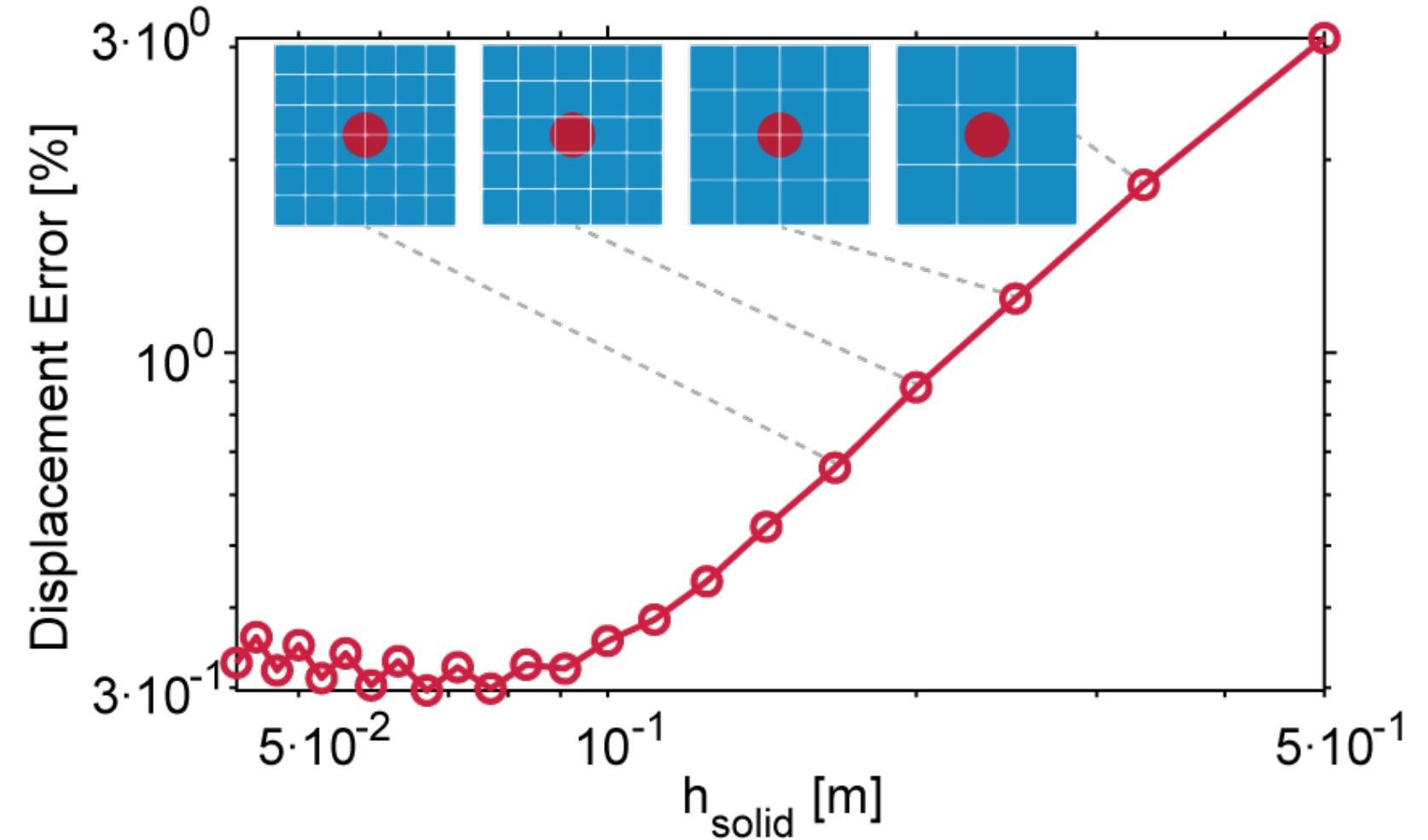
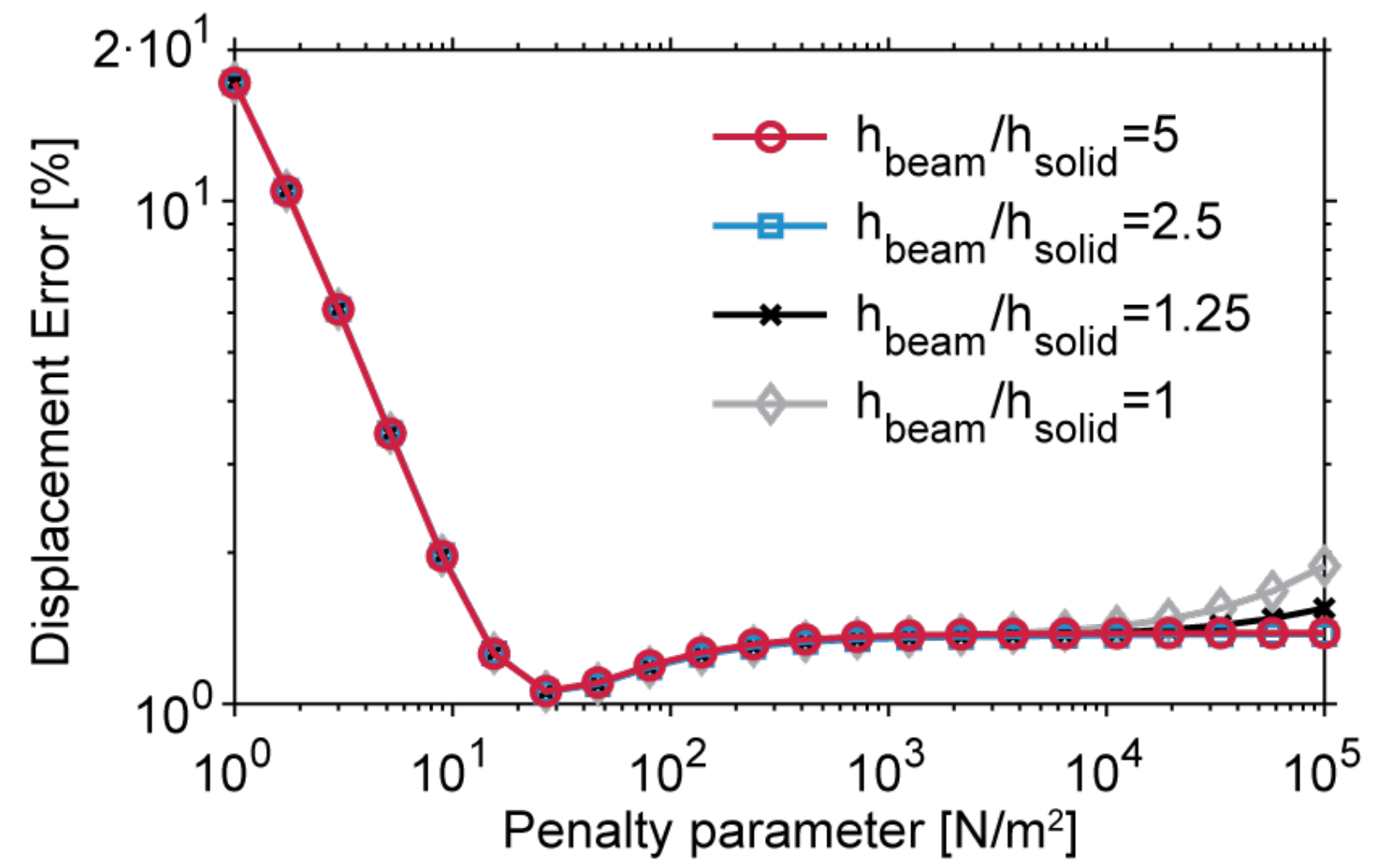
- Reference solution

- Solid elements: 75,985
- CPU time: 2210 sec



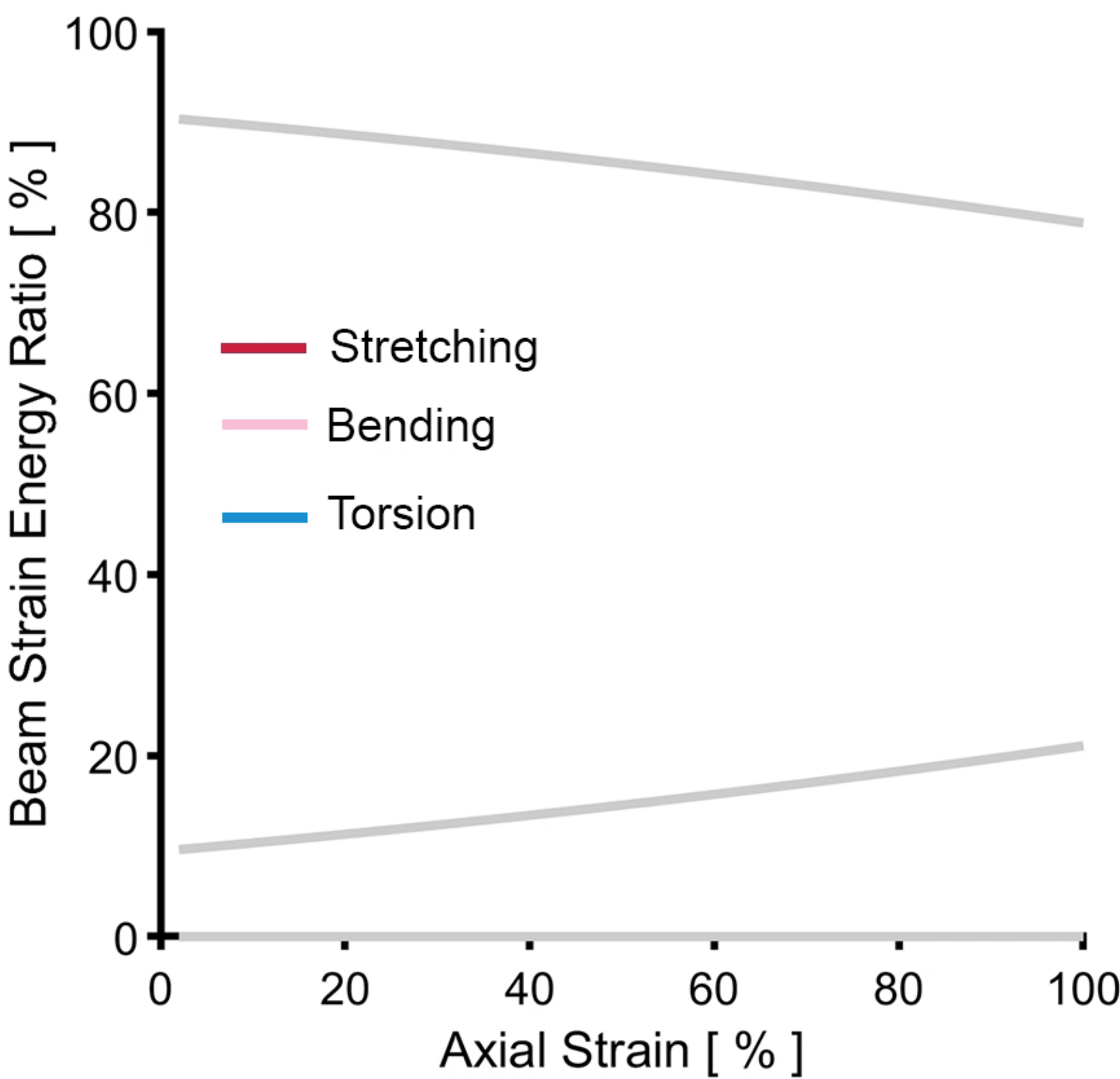
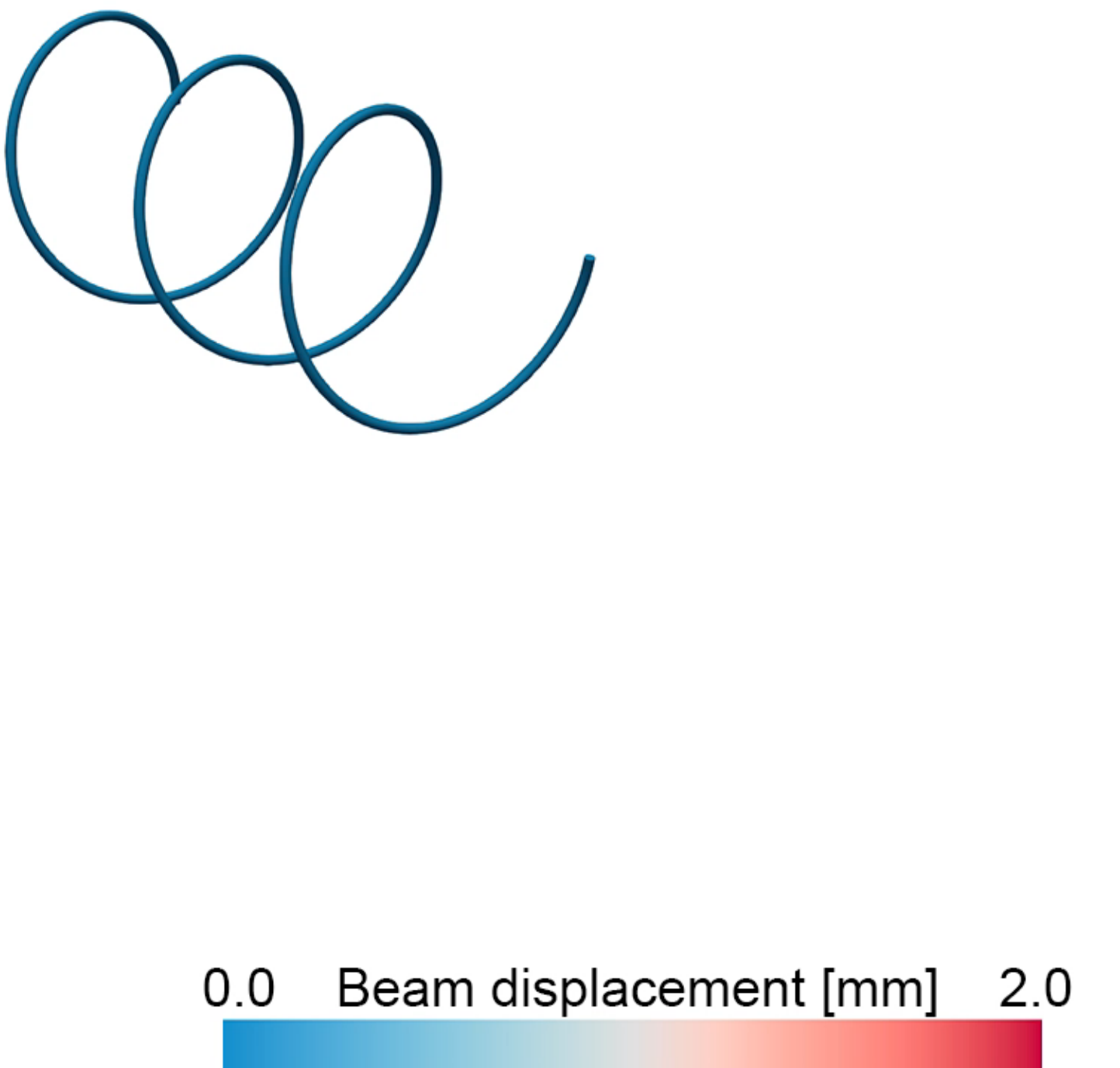
- Beam-to-solid coupling

- Solid elements: 625
- CPU time: 29 sec



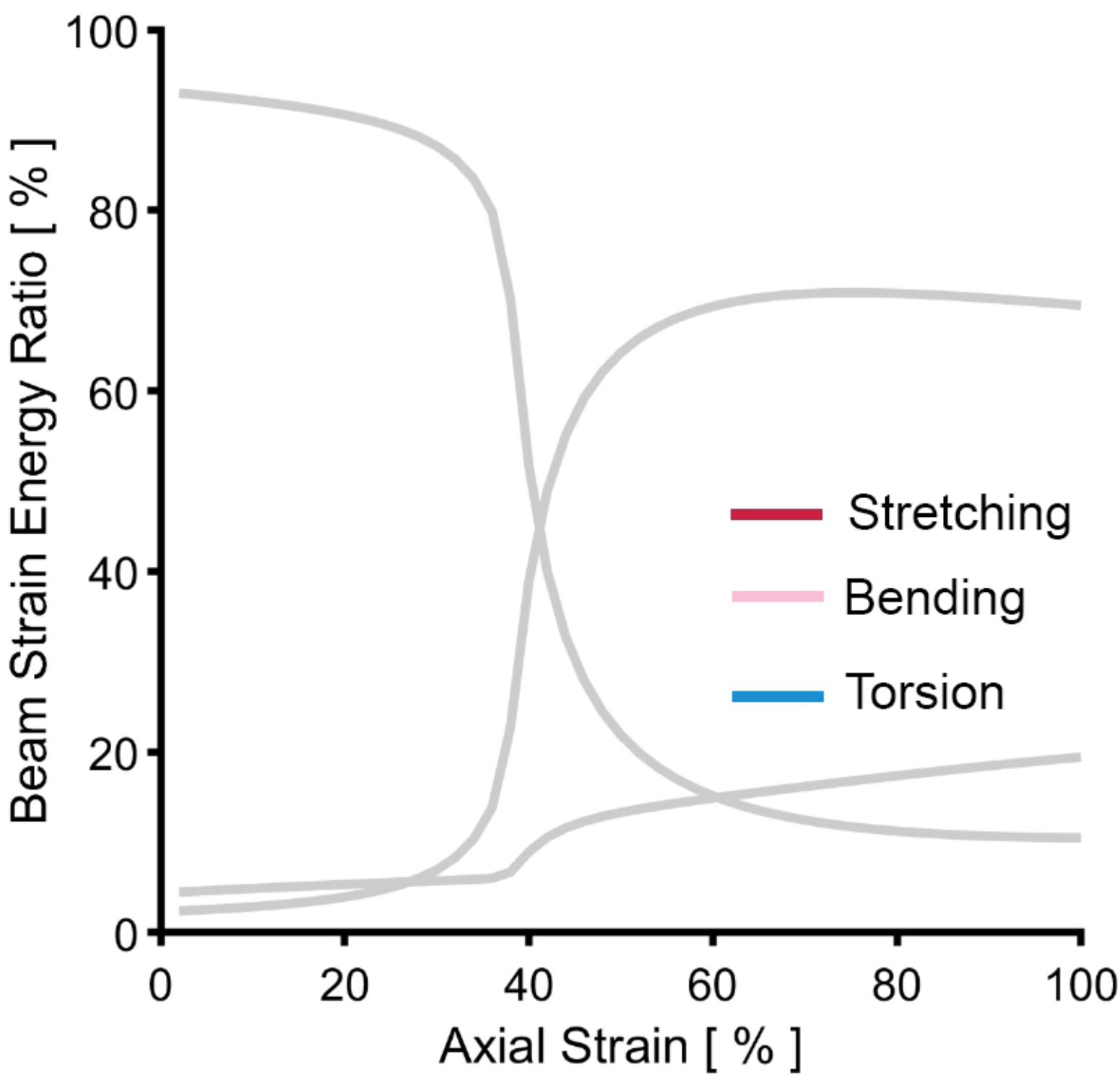
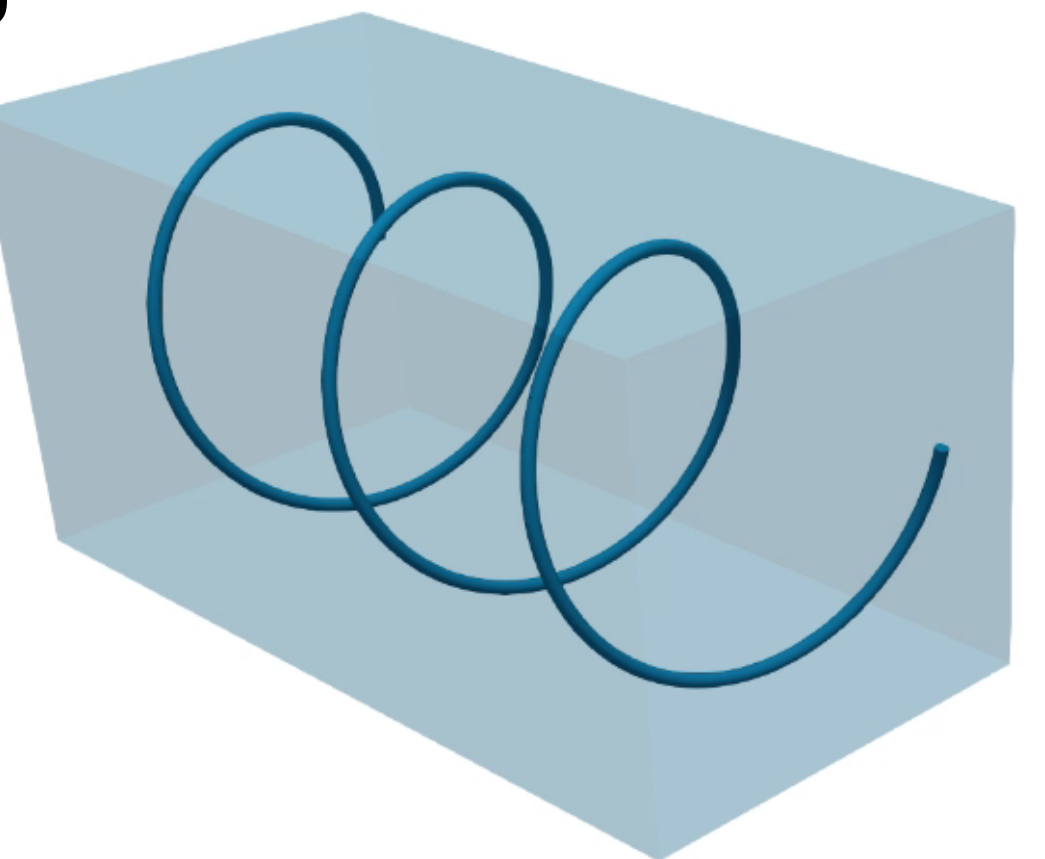
Example: Helical Beam

- Spatial Timoshenko beam.
- Linear elastic material law.
- Uniaxial extension to 100% strain.
- Strain energy components:
 - Axial stretching
 - Bending
 - Torsional



Example: Helical Beam

- Same beam, embedded into isotropic, incompressible Neo-hookean material.
- Our model is able to:
 - Capture beam instabilities caused by the solid-to-beam interaction forces.
 - Delineate the contribution of each strain energy component.
 - Investigate the effect of the relative stiffness between the solid matrix and the beam.



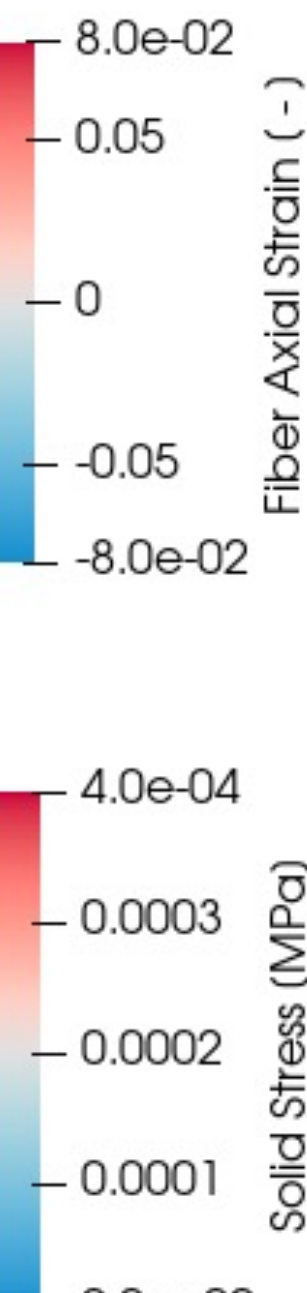
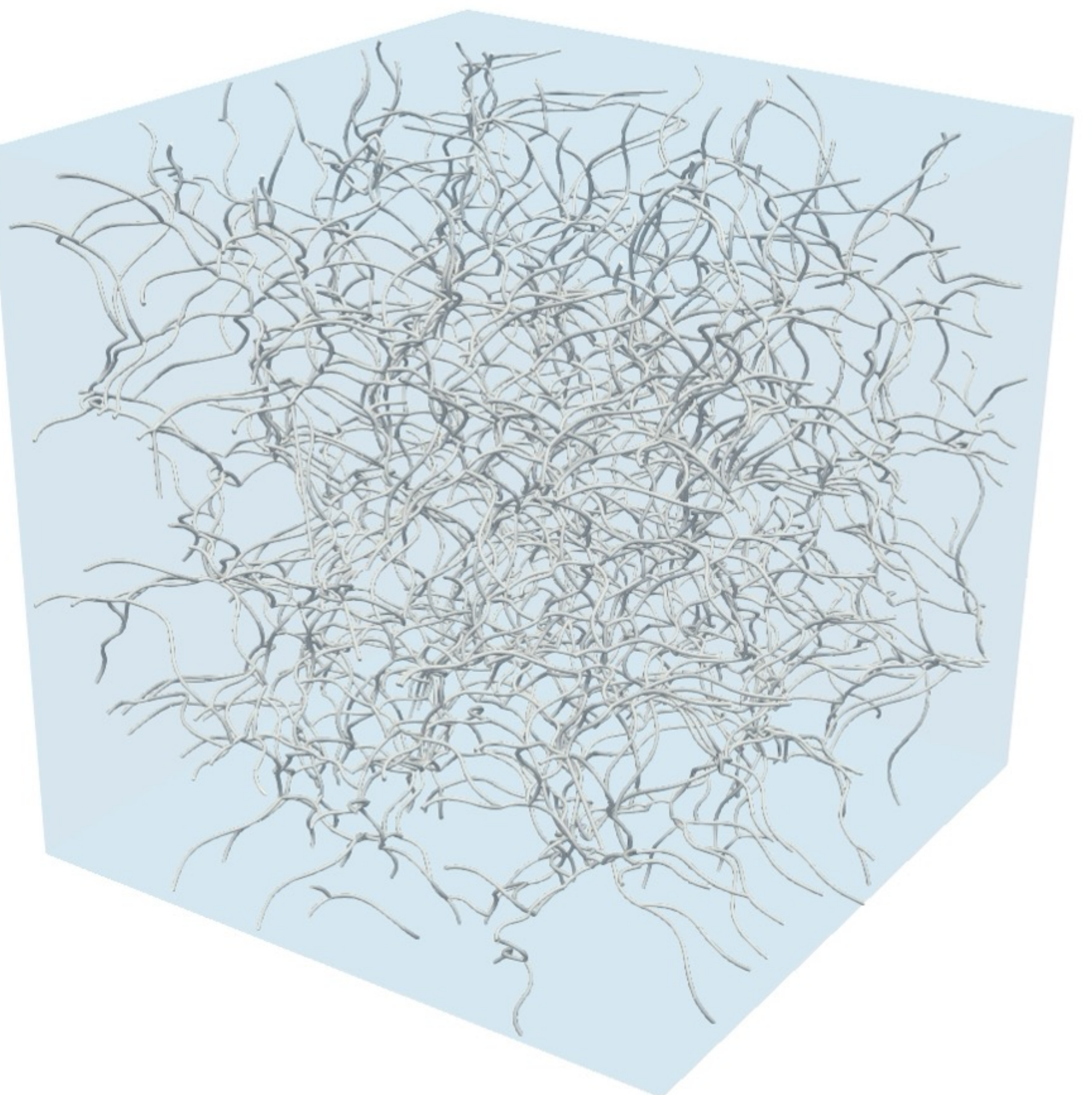
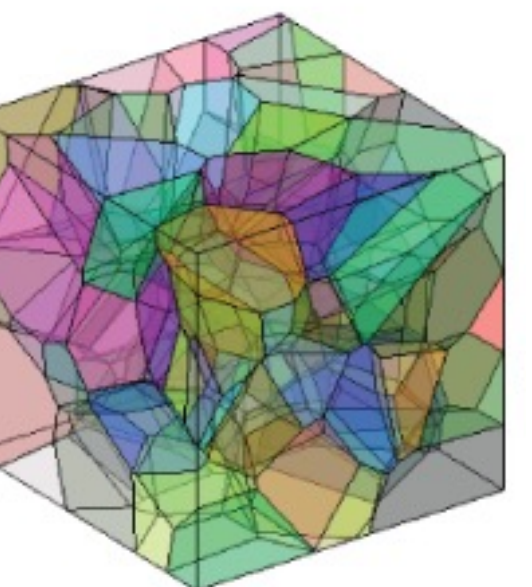
Embedded Fiber Networks

- Voronoi-based networks
 - Average connectivity number $\langle z \rangle = 3.4$
 - Introduce sinusoidal undulations

- Simple shear deformation
 - Rigid displacement boundary conditions
 - Cubic geometry
 - Deformed up to 50% shear strain

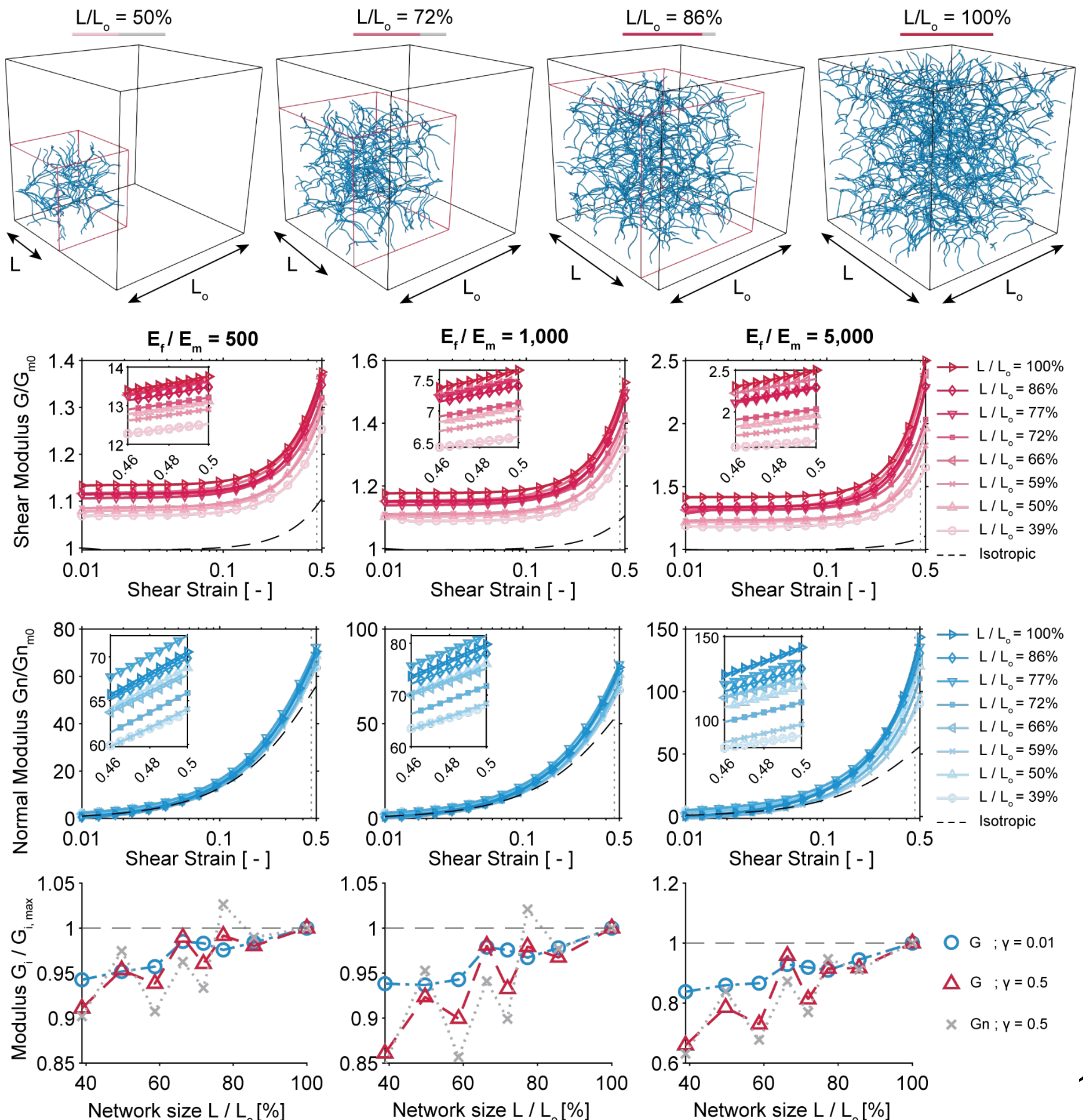
- Effective Stiffness
 - Shear & Normal moduli

$$G = \frac{\Delta\sigma_{xy}}{\Delta\gamma}, \quad G_n = \frac{\Delta\sigma_{yy}}{\Delta\gamma}$$



Size Effect

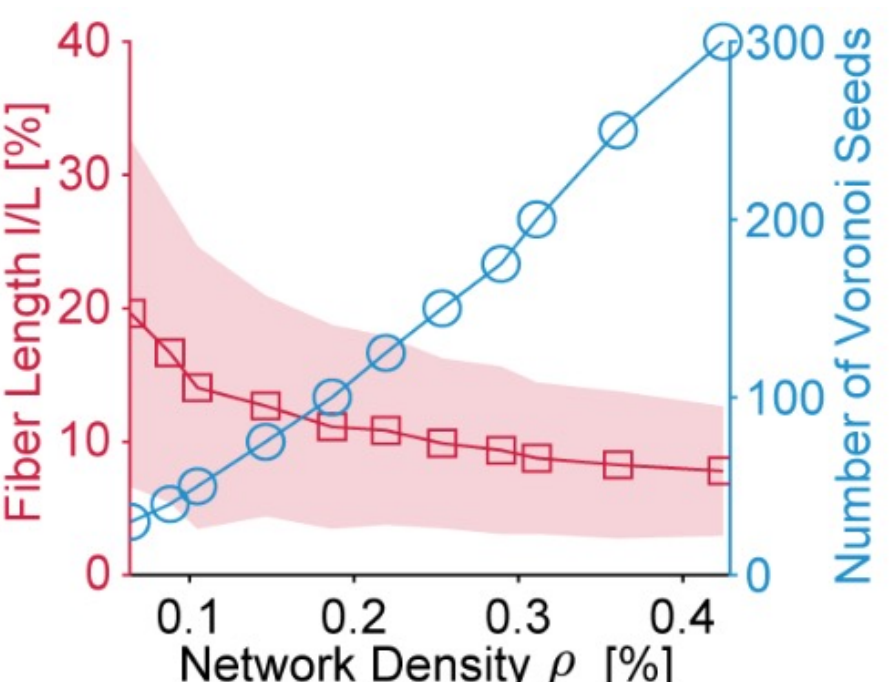
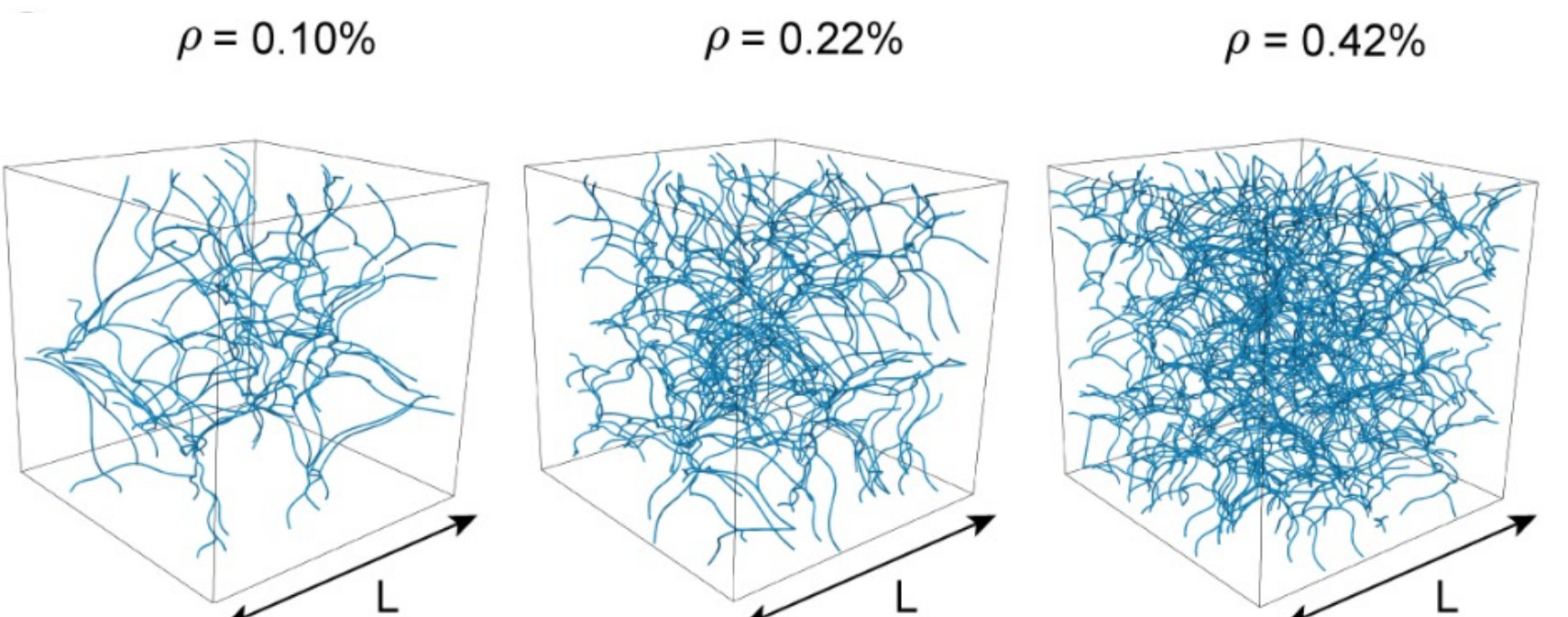
- Investigated the size effect on the apparent stiffness
 - Varying network sizes with same density
 - Shear Modulus
 - Normal Modulus
 - At three different fiber-to-matrix stiffness ratio E_f/E_m
- The size effect is more prominent at
 - Higher fiber-to-matrix stiffness ratio
 - Shear modulus at the low-strain regime
- Highest density network converges sufficiently for both Shear and Normal moduli
 - Increasing fiber number the change in effective moduli decreases



Density Effect

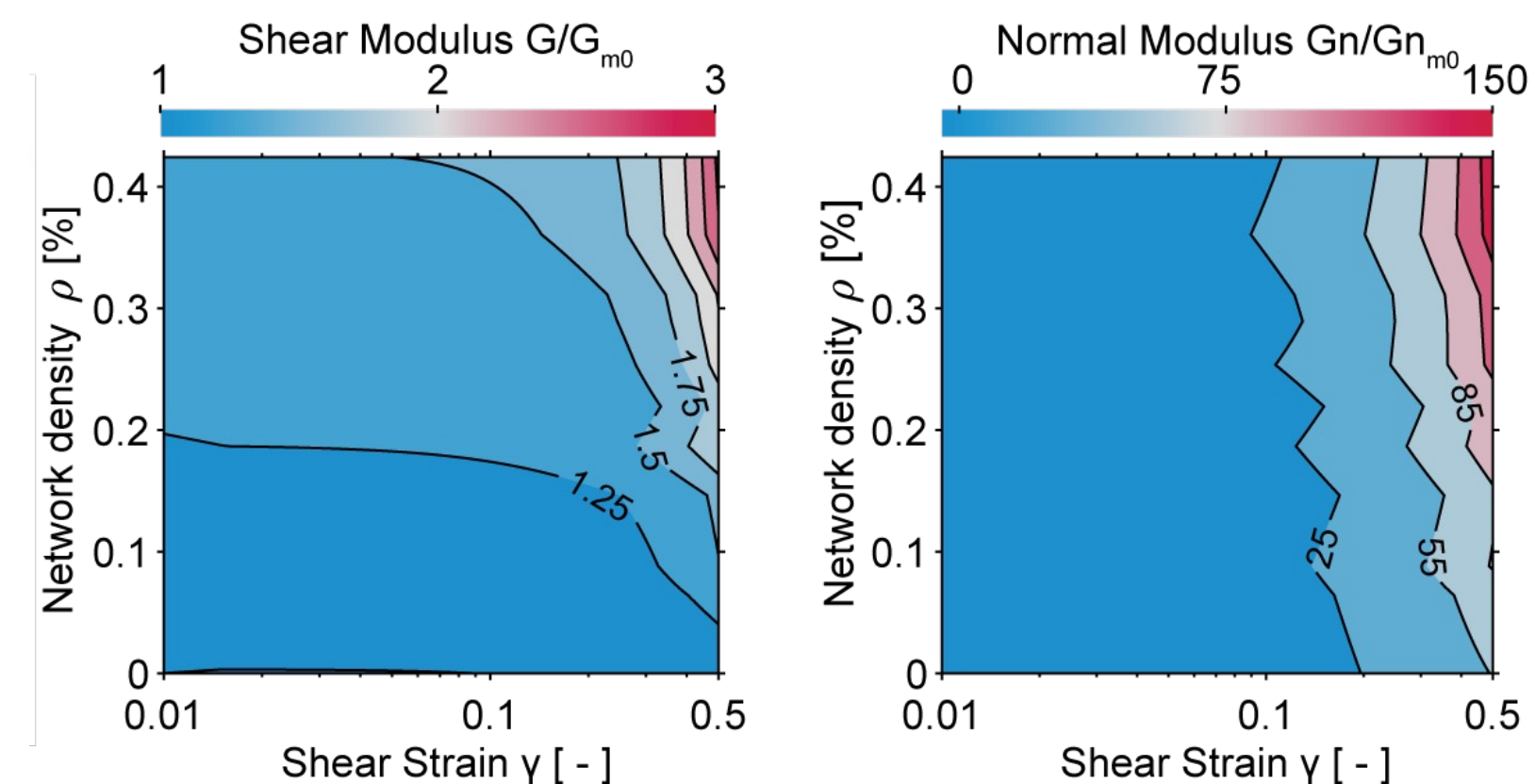
■ Network Density Study

- Constant network size (edge length)
- Decreasing mean fiber length
- Increasing network density
- Simple Shear deformation

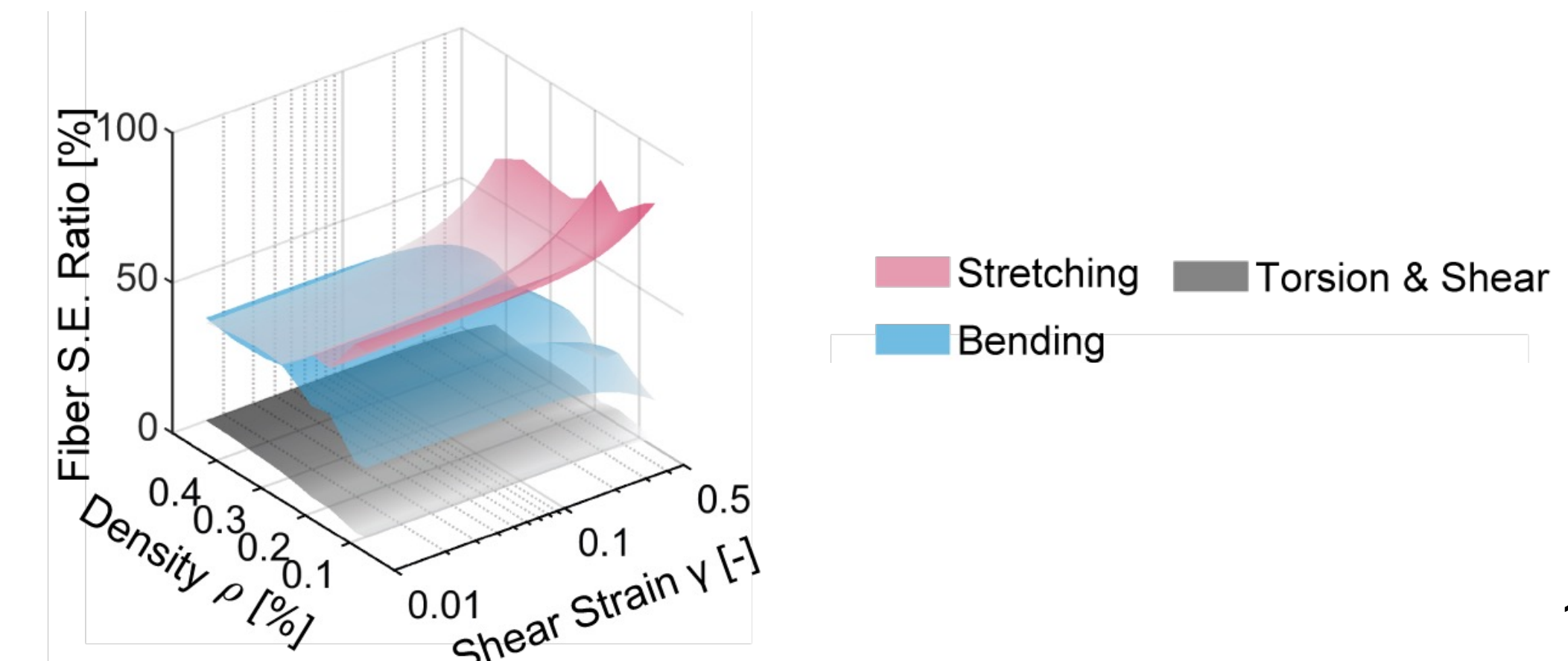


■ Embedding fiber networks leads to

- Strain stiffening behavior
- A more pronounced negative Poynting effect

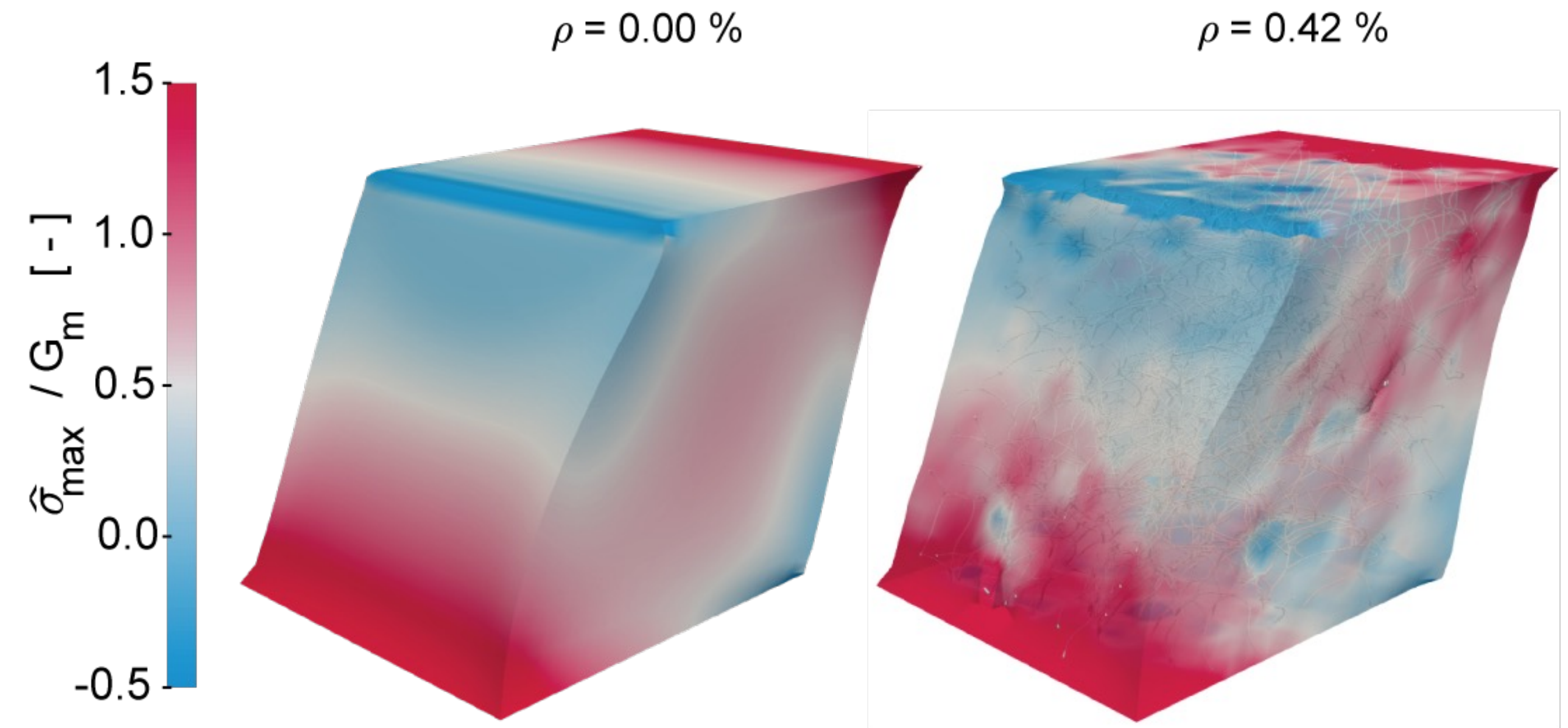
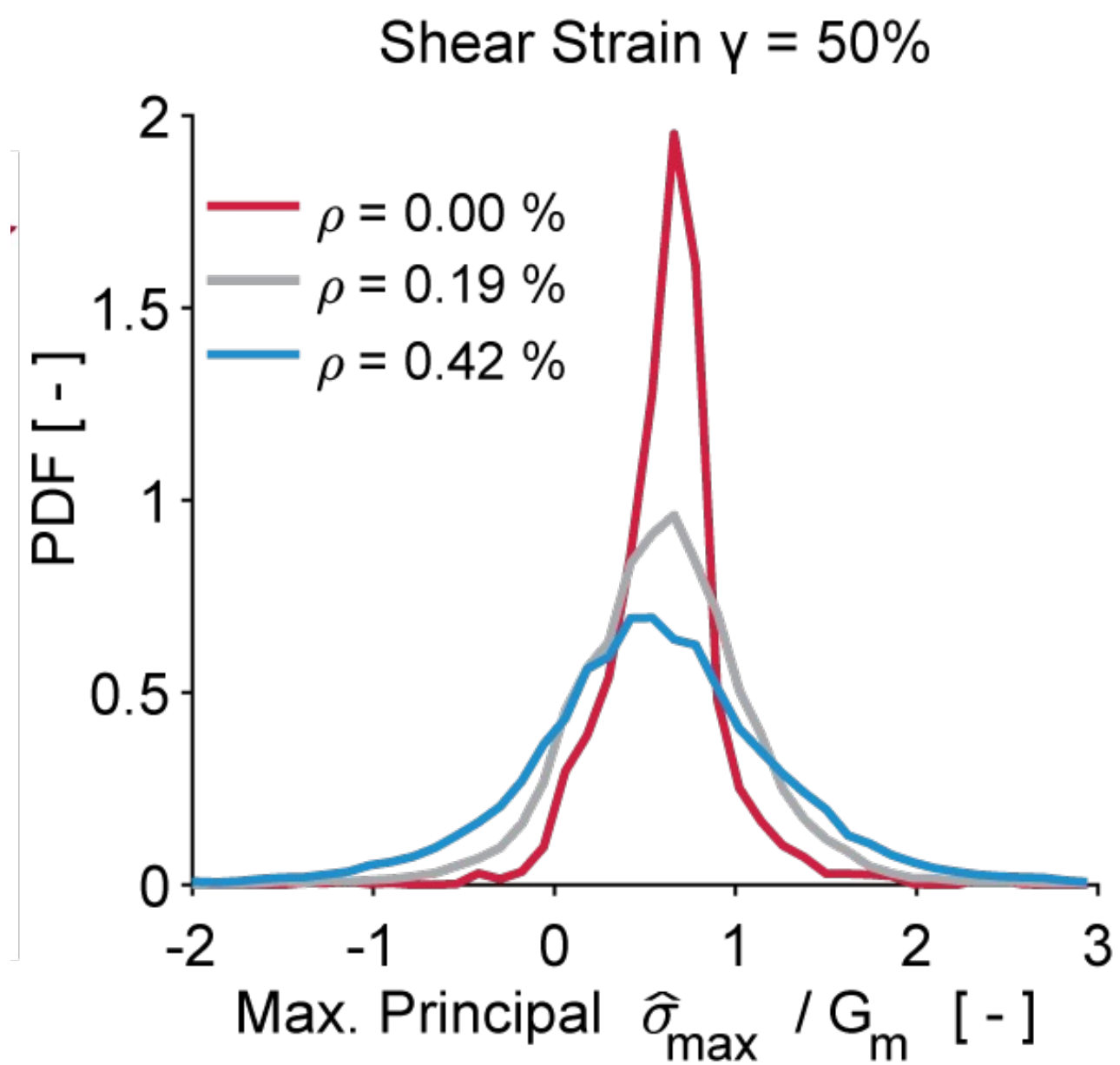


■ From a strain energy perspective, these phenomena are driven primarily by fiber stretching, rather than bending or torsion



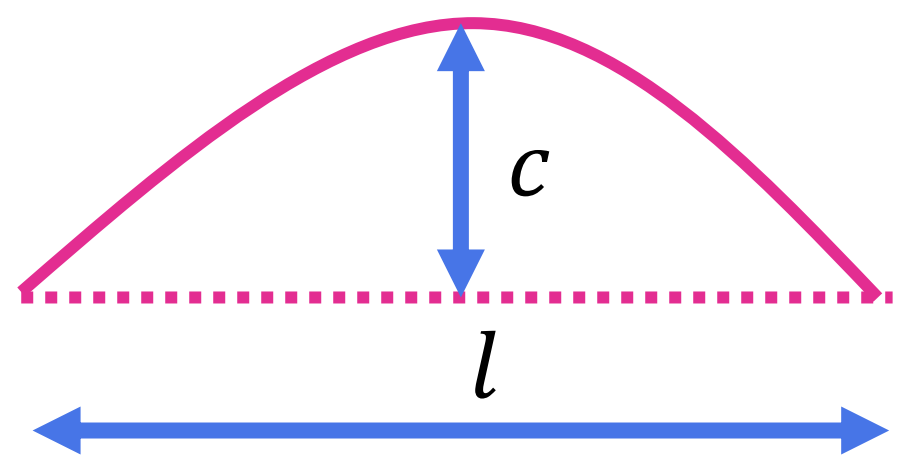
Networks and Matrix-stress Distribution

- Distribution of max. principal stress as a function of network density
- Embedding networks introduce
 - Stress heterogeneity
 - Local stress concentrations

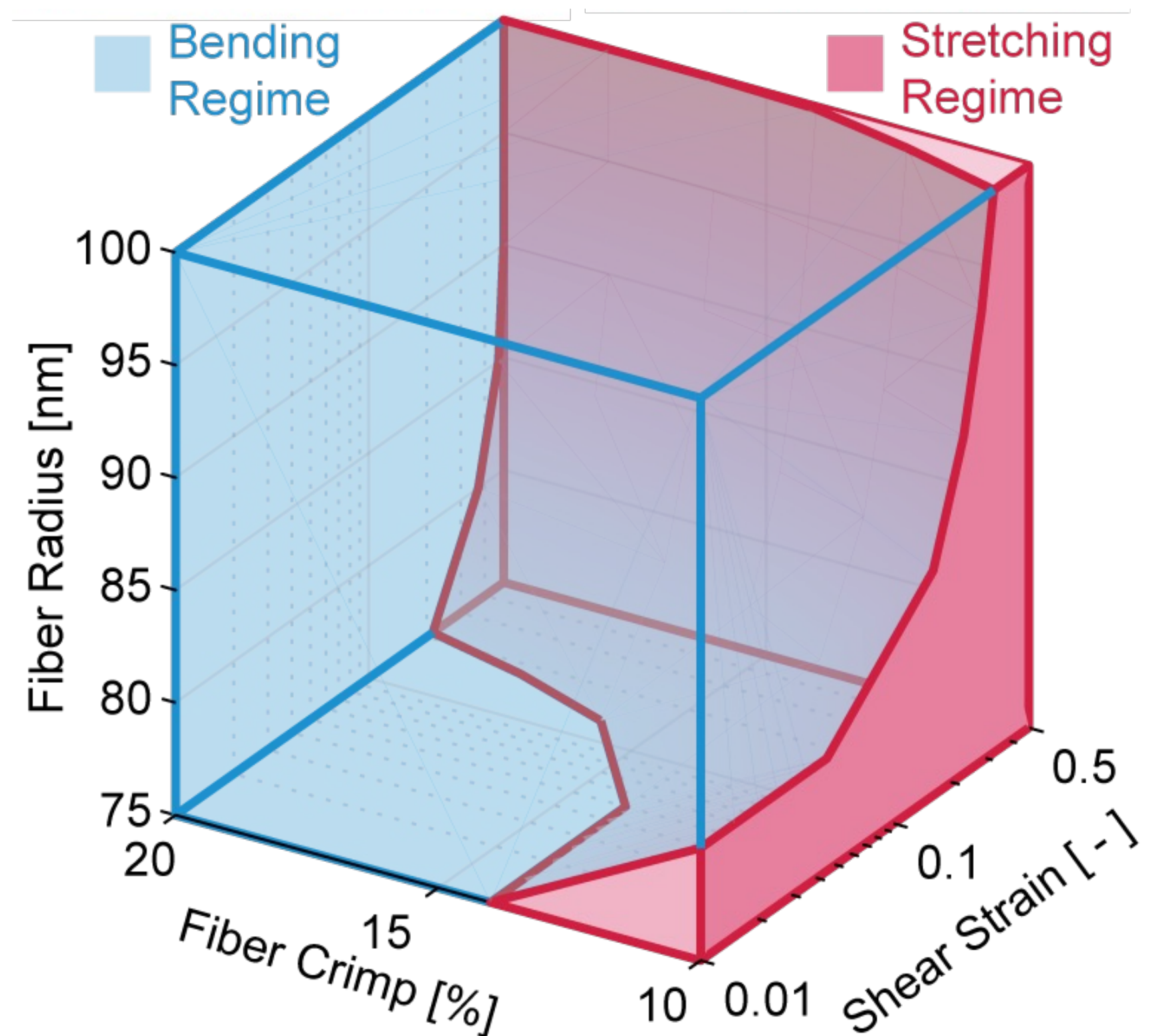
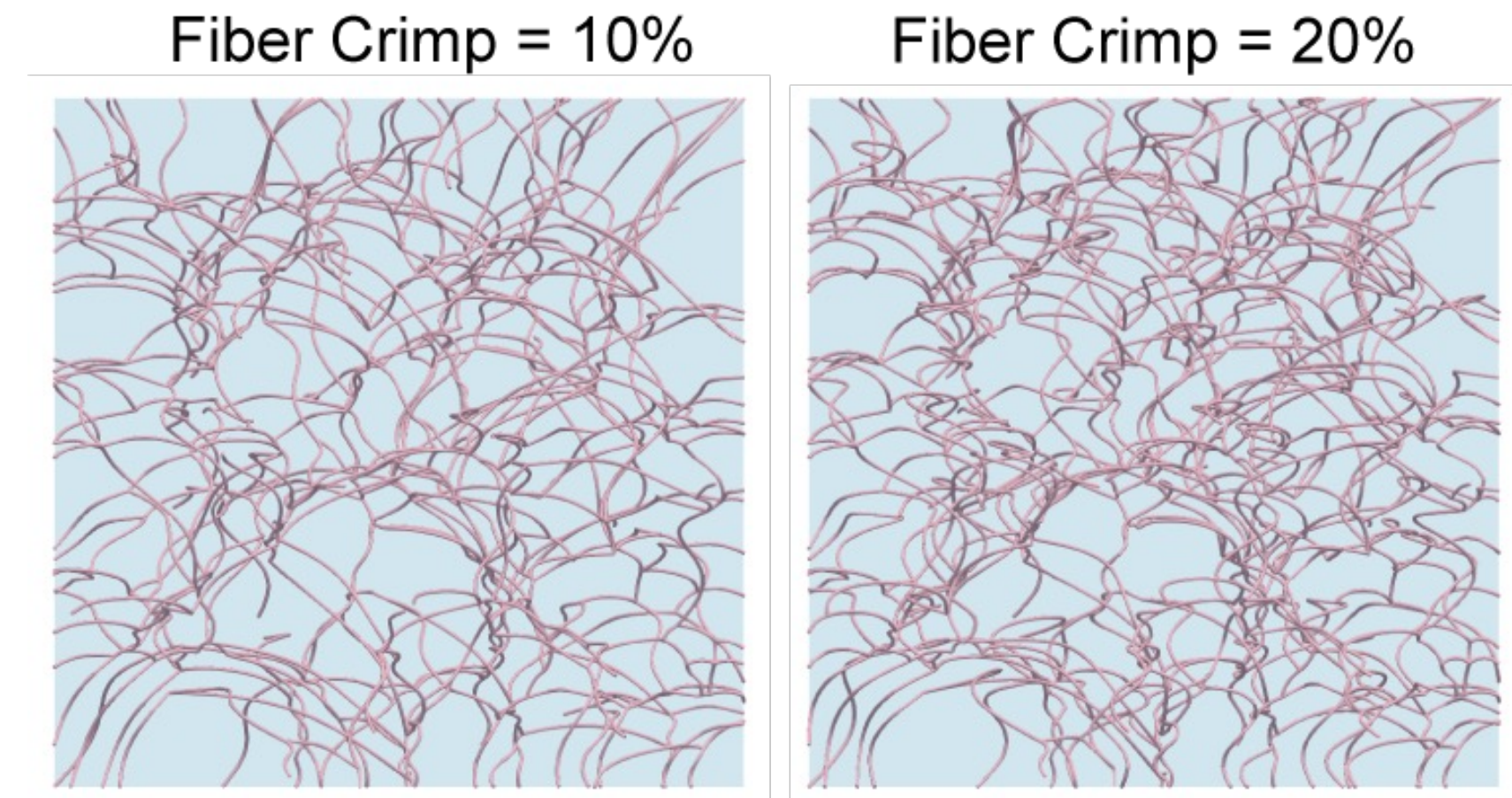


Fiber Strain Energy

- Fiber crimp c/l [%] & fiber radius

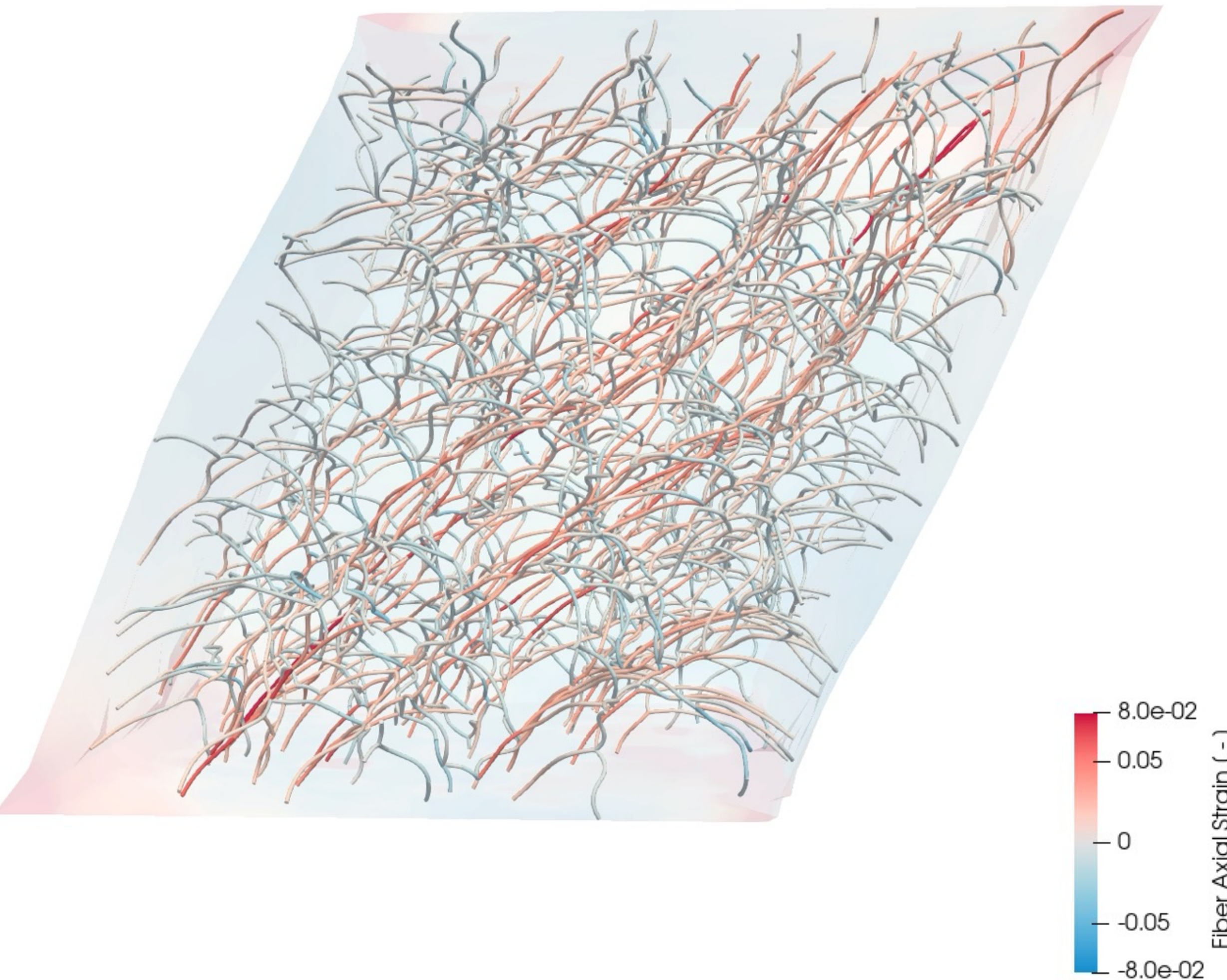


- Stretching energy dominates for
 - Large deformations
 - Fibers with small undulations
 - Fibers with small radii
- Bending energy dominates for
 - linear/small deformations
 - fibers with large undulations
 - fibers with large radii



Conclusion

- Given the limitations presented (penalty parameter, mesh size, element length ratio), the mortar-type finite element approach can provide efficient models for embedded fiber networks.
- Embedding fiber networks leads to
 - Strain stiffening behavior
 - Negative Poynting effect
 - Stress heterogeneity
- Stretching (membrane) strain energy dominates the mechanics at large deformations.
- Future work
 - Interpret experimental data (blood clot modeling).
 - Expand on viscoelastic and/or damage-failure models of the fibers.



THANK YOU.

Dr. Manuel Rausch

**SOFT TISSUE
BIOMECHANICS
LABORATORY**



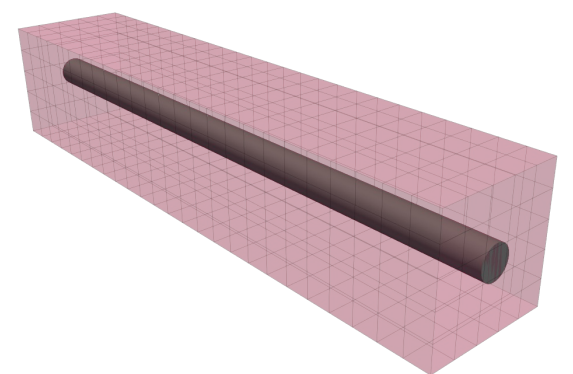
The University of Texas at Austin
Aerospace Engineering
and Engineering Mechanics
Cockrell School of Engineering





The University of Texas at Austin
Aerospace Engineering
and Engineering Mechanics
Cockrell School of Engineering

Theory



- Discretization of the solid, beam displacement and the Lagrange multiplier (LM) fields:

$$\underline{\mathbf{u}}_h^S = \sum_{k=1}^{n_S} N_k(\xi, \zeta, \eta) \mathbf{d}_k^S$$

$$\underline{\mathbf{u}}_h^B = \sum_{l=1}^{n_B} H_l(\xi^B) \mathbf{I}^{3x3} \mathbf{d}_l^B$$

$$\underline{\lambda}_h = \sum_{l=1}^{n_\lambda} \Phi_j(\xi^B) \lambda_j$$

- Coupling matrices from δW^C (integration on the beam centerline):

$$\mathbf{D}^{(j,l)} = \int_{\Gamma_{c,h}^B} \Phi_j H_l(\xi^B) ds \quad \mathbf{I}^{3x3}$$

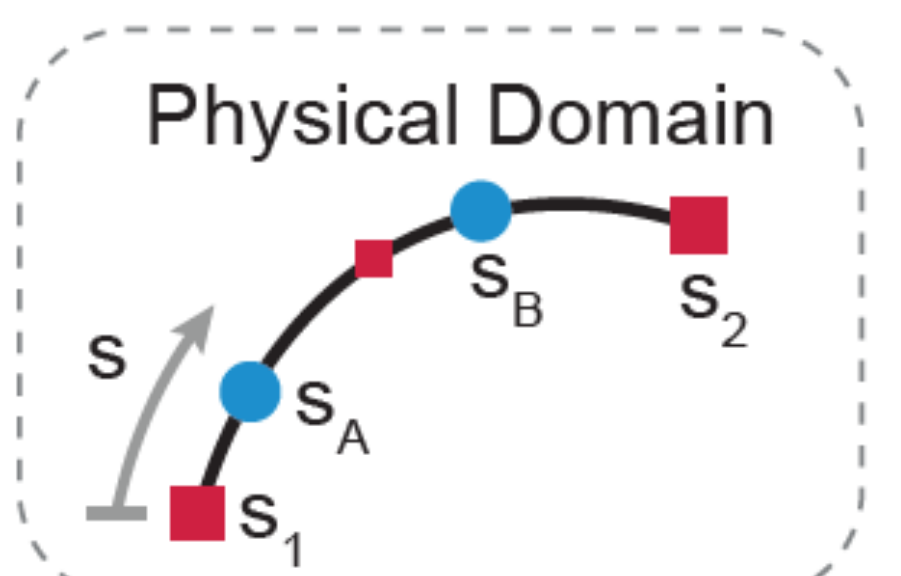
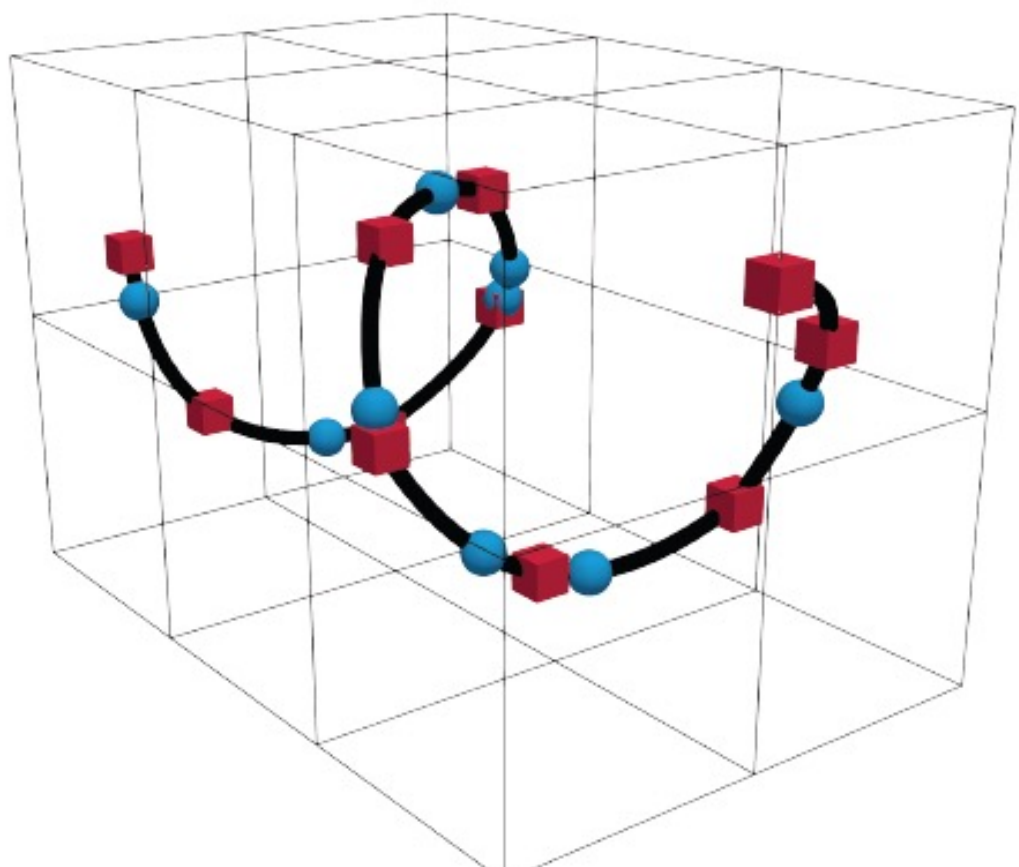
LM node $j \leftrightarrow$ Beam node l .

$$\mathbf{M}^{(j,k)} = \int_{\Gamma_{c,h}^B} \Phi_j N_k ds \quad \mathbf{I}^{3x3}$$

LM node $j \leftrightarrow$ Solid node k
Projection to solid domain to evaluate N_k

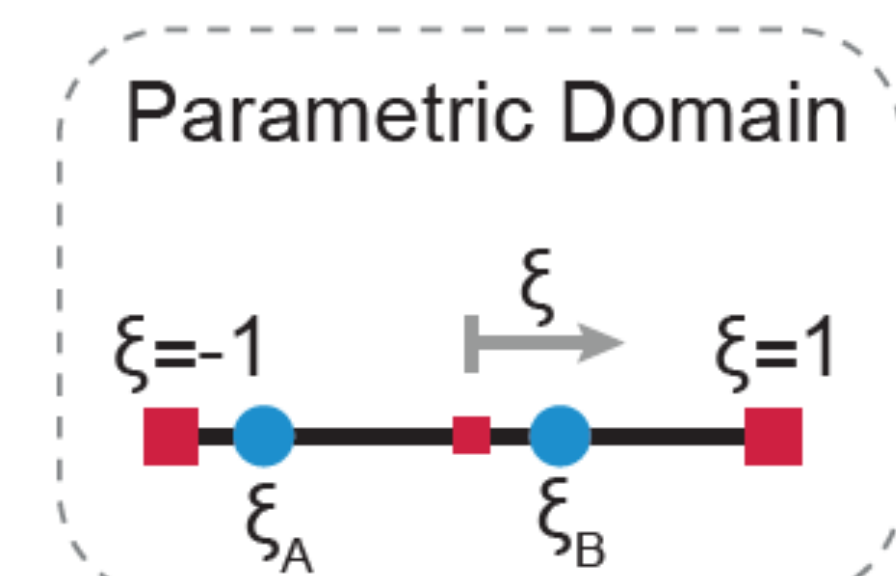
$$\boldsymbol{\kappa}^{(j,j)} = \int_{\Gamma_{c,h}^B} \Phi_j ds \quad \mathbf{I}^{3x3}$$

Scaling matrix: LM node j



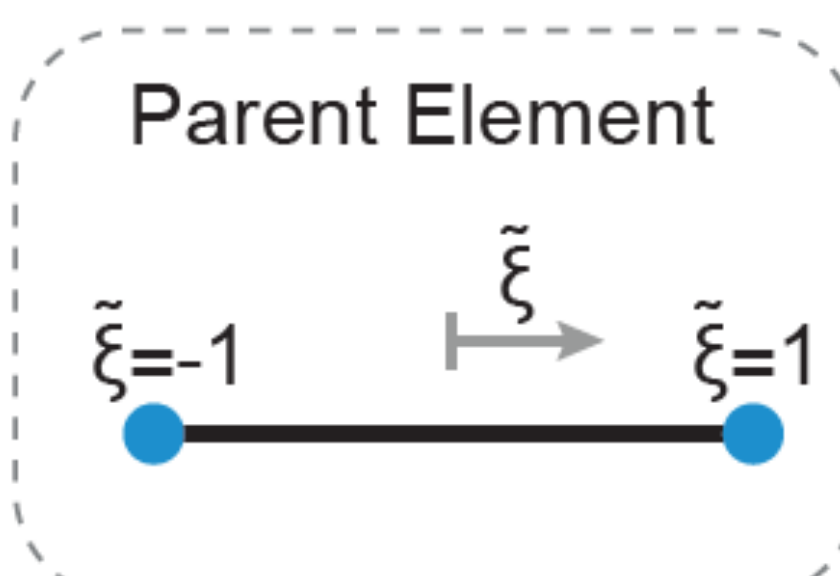
■ Element Node

$$ds = J_A d\xi$$



● Segment End Point

$$d\xi = J_B d\tilde{\xi}$$

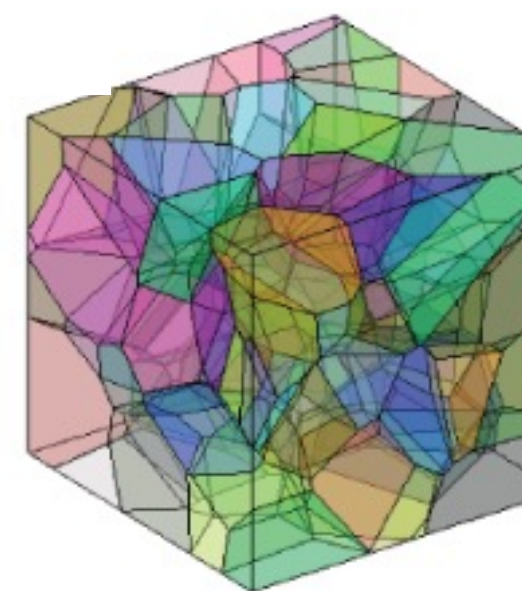


— Beam Domain

Embedded Fiber Networks

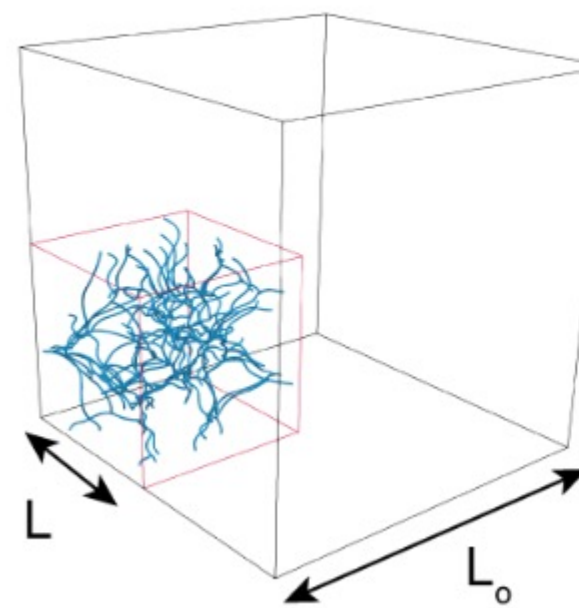
- Voronoi-based networks

- Average connectivity number $\langle z \rangle = 3.4$
- Introduce sinusoidal undulations

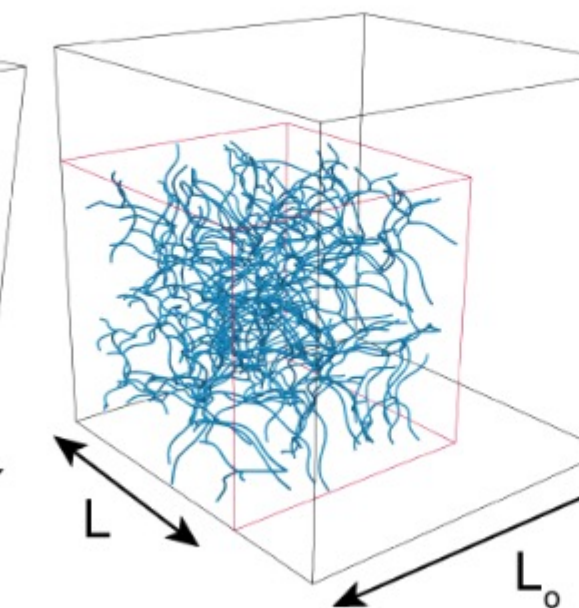


- Size Effect Study

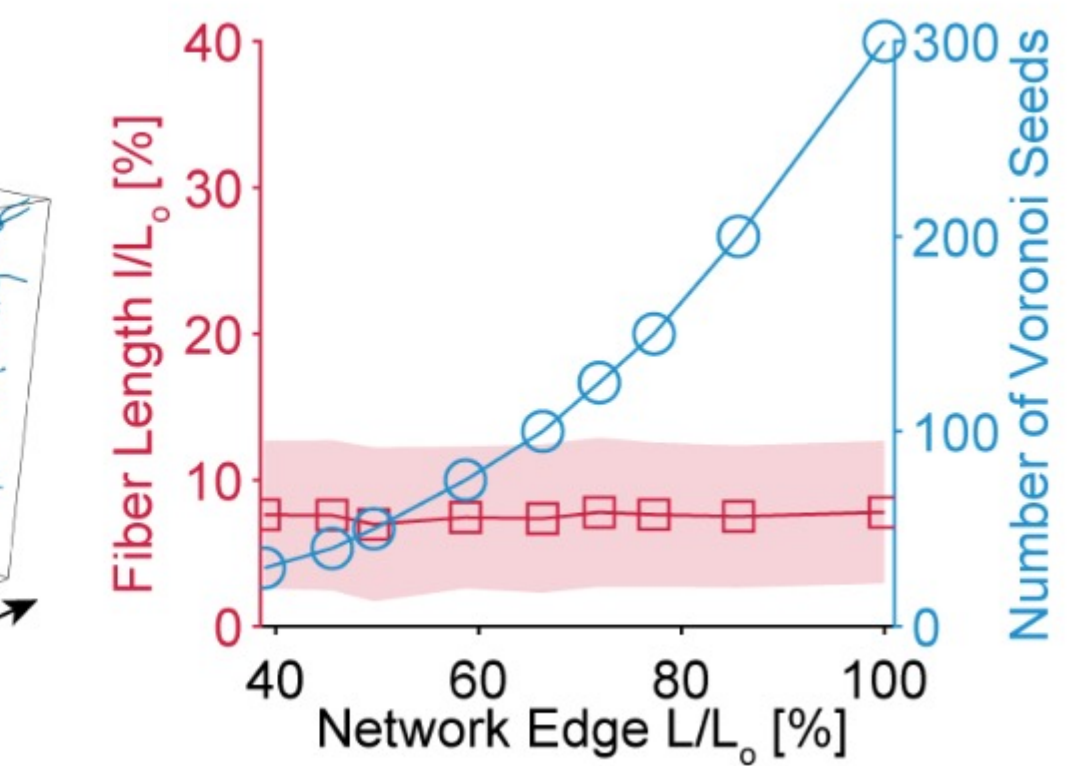
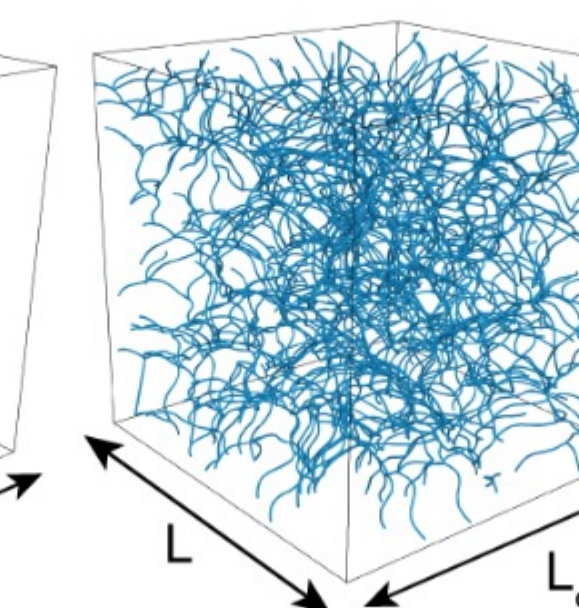
$L/L_o = 50\%$



$L/L_o = 72\%$

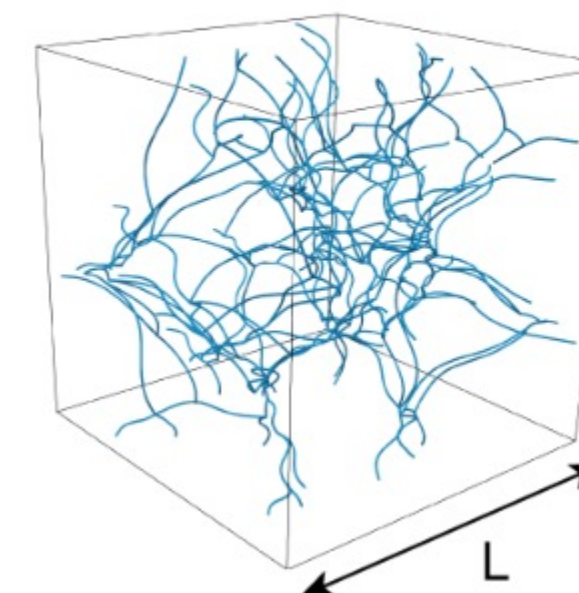


$L/L_o = 100\%$

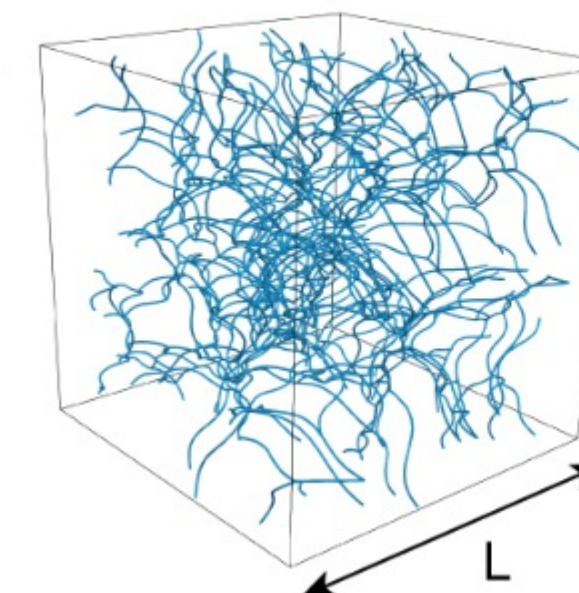


- Density Effect study

$\rho = 0.10\%$



$\rho = 0.22\%$



$\rho = 0.42\%$

